2018

Investigation and Identification of Dye Structure as a Function of Solvent and Temperature

Uncles, C.F.

Uncles, C.F. (2018) 'Investigation and Identification of Dye Structure as a Function of Solvent and Temperature', The Plymouth Student Scientist, 11(2), p. 244-308.
http://hdl.handle.net/10026.1/14190

The Plymouth Student Scientist
University of Plymouth

Investigation and Identification of Dye Structure as a Function of Solvent and Temperature

Caroline Fiona Uncles

Project Advisor: Roy Lowry, School of Geography, Earth and Environmental Sciences, University of Plymouth, Drake Circus, Plymouth, PL4 8AA

Abstract

Triarylmethane dyes have absorption spectra that contain two peaks which overlap in polar solvents. The second peak being described as a shoulder peak. The body of work recorded in this dissertation aims to discover which of the theories behind the shoulder present on these absorbance spectra holds most precedence. Stock solutions of 5 different dyes with a range of steric factors and symmetries were prepared to a concentration of 10^{-3} M in 5 different solvents. These were primary, unbranched alcohols with chain lengths of C_1 to C_4 and water. The stock solutions were diluted to a concentration of 10^{-5} M, before analysis. The absorbance spectra, were obtained at room temperature, then between the ranges of 0-10°C, 10-20°C, 30-40°C and 40-50°C. In total, 125 different spectra were recorded plus an additional 30 spectra to characterise the uncertainties in the experimental procedure. Graphs of the difference in the λ_{max} and the secondary peak ($\Delta\nu$) in wavenumbers against the solvatochromic parameters α, β and π* were plotted. These graphs indicate that the solvent was interacting with 4 of the dyes via inducing dipoles in dye and hydrogen bonding. Victoria blue R interacted with the solvent by hydrogen bonding too, though the hydrogen comes from the dye rather than the solvent. It was found that the number of auxochromes and if they were sterically hindered would impact how strong the hydrogen bond interaction was and change the degree of splitting. A decrease in temperature would decrease the splitting between the 2 peaks also. The interaction between the dye and solvent causes a decrease in the dye symmetry. This is shown on the absorption spectra as a shoulder peak at the shorter wavelength side. The cause of the reduction in symmetry of the dyes is by the interaction of the solvent with the dye.

Introduction

Triarylmethane dyes have many technological applications and are used throughout several industries (1). They are more commonly found within the textile industry as dyes used for silk, cotton and wool (2). They are also used in the preparation of inks and as colourants in food and drug manufacturing (1). The dyes can also be found being used in the veterinary industry as well as biological stains (1). More recently, they have been considered as photosensitizers in dynamic phototherapy (3).

Triarylmethane dyes are known by a wide variety of names due to the four separate systems of nomenclature that exist. These include: colour index, CA index (CAS registry number) and the IUPAC naming method, as well as commercial/trivial names (4). The terminology “triarylmethane” has been used throughout this study, though triarylmethane and triphenylmethane class names can be used. Although the report uses the name triarylmethane, the name itself is misleading due to the central carbon atom been sp^2- hybridized and not sp^3-, therefore a more systematic way of naming the class would be as triarylmethine (5). Triarylmethane dyes are split into three sub categories; (a) pigment derived from basic dyes, (b) pigments derived from acidic dyes, and (c) alkali blue (2). The dyes considered as part of this study are from category (a) pigments derived from basic dyes. This category can further be split into three main types of dye categories: rhodamines, methyl violets and Victoria blues (2).

The structural determination of the dyes is important due to the commercial/trivial naming system, as structures often vary between manufacturers using the same dye name (2). One of the important first steps after purification is to determine the UV-vis spectrum (2). UV-visible spectrophotometry, although not known for its use to determine structure, provides a great deal of information about the triarylmethane dyes (2). However, for UV-visible spectrophotometry to yield useful data the compound must exhibit a colour. Typically, dyestuffs have excellent brilliance and colour strength though they may also have poor durability, poor heat and solvent stability (6). The colour is due to the electronic properties of the chromophore part of the molecule (6). The chromophore structure present in the triarlymethane dyes is shown in Figure 1, (6).

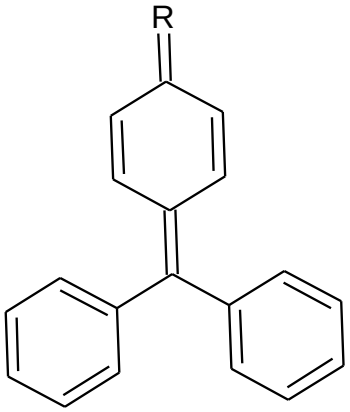

Figure 1: Chromophoric group present in triarlymethane dyes.

The R in Figure 1, denotes a side chain, these side chains tend to involve auxochromes. Auxochromes, are functional groups containing lone pairs of electrons which modify the light absorption of the chromophore (7). The auxochrome involved in triarlymethane dyes tends to be nitrogen and this is the case for the 5 dyes selected for this study.

For the colour to be perceived, a compound must exist in the ground state and then be raised to an excited state by visible radiation (8). Which occurs in the wavelength range of 400 -750 nm (5, 9). Colour vison in the human eye is based on physical, chemical, and physiological processes (5) and the perception of colour by the human eye depends on the position of the band and shape of the band in a spectrum (5, 9). Other important spectral characteristics include the intensity of the band and the polarizability of the band (9). The perceived brightness of the dye depends on its ability to fluoresce (10).

The wavelengths absorbed by a dye (the visible absorption spectrum) can be determined through the use of UV-vis spectrophotometry. Currently 3 types of instrument exist under the category of spectrophotometry these are; single beam spectrophotometer, double beam spectrophotometer and photodiode array spectrophotometer. UV-visible spectrophotometry is commonly used for qualitative and quantitative work in analytical laboratories (11). Certain performance characteristics will affect a scanning spectrophotometer, like the single or double beam, more than a diode array (11).

A single beam instrument measures the light transmitted by the sample as a function of wavelength (12).In order to obtain a wavelength scan the using a single beam instrument a tedious process is undertaken as the wavelength must be set then instrument blanked before the sample absorbance value is obtained (13). Although, some single-beam spectrophotometers have a rapid scanning capability this is where a motor is used to rotate the grating at the same time as absorbance readings are recorded (13).

A double beam spectrophotometer compares the light energy through a sample with that going through a reference cell (12). The two light beams allow for the instruments software to automatically adjust for the blank at each wavelength (13).

A photodiode array is able to simultaneously observe all wavelengths in the range 190-1100 nm and the information can be acquired in milliseconds (14). Whereas the single and double beam instruments (whilst in scanning mode), obtain the information by scanning across a wavelength range (14). This is done by using a continuous source lamp of deuterium (or tungsten) and a dispersive element such as a prism or grating (14). The dispersive element is rotated to change the wavelength of light passing through the exit slit and then into the sample before been detected by photomultiplier tubes (14).

There are many factors which influence UV-vis spectra of dyes, these include the chemical environment and steric effects as well as pH of the solution (4).

The main advantages of a double beam instrument include better resolution and stability (11). However, the advantages of the diode array instrument include speed of measurement scan acquired and the ruggedness of the instrument in wavelength accuracy (11).

Single beam and diode array instruments only require a single cuvette, the double beam requires two. These two cuvettes have to be optically paired or "matched" (13, 15). Matched cuvettes for the double beam are identical with regards to the path length, reflective and refractive properties (13). The cuvette should be placed in the instrument in the same rotation each time this ensures that the reflective and refractive properties do not change and cause an error in the result (13). Cuvettes used in UV-visible spectrophotometry must be transparent at all the wavelengths under study (13). When using visible light the cuvette must be completely clear and colourless and typically the material is glass although plastic can also be used (13). Glass and plastic are not transparent in the ultraviolet section of the electromagnetic spectrum so instead quartz cuvettes can used (13). A quartz cuvette is more expensive than the plastic or glass cuvettes (13).

The absorption spectra of conjugated molecules can be predicted by theoretical modelling (9) which can also determine the extinction coefficient of the dyes (5). The extinction coefficient (or molar absorptivity), is a measure of how much light a chemical species absorbs at a given wavelength. It can be expressed according to the Lambert-Beer law (5):

$$\log \frac{I_0}{I} = A = \varepsilon\, d\, c$$

Where I, is the intensity of light after passing through the sample and I_0 is the intensity of light before entering the sample, A is the absorbance, ε the extinction coefficient, d is the path length, and c the concentration. The extinction coefficients, ε, are a characteristic of the absorbing material (16). Triarlymethane dyes are known to have high extinction coefficients, in the range of ε ≥100,000 L mol^{-1} cm^{-1} (5). These dyes are deemed to be more economical, compared to other dyestuffs, as the cost is increased due to low extinction coefficient values and hence the need to use more dyes to obtain a particular depth of colour (5).

Triarlymethane dyes exhibit interesting UV-vis absorption spectra, due to the presence of a second absorbance band (5). This second absorbance peak is deemed to be a "shoulder" due to being heavily overlapped by another more intense absorbance band (17). The secondary band is unresolved in polar solvents and is resolved in non-polar ones (17).

Five different theories exist in order to explain the occurrence of the secondary absorbance band seen on the spectra of triarylmethane dyes. These theories are isomers, symmetry, aggregation, ion-pairing and transitions along the x- and y- axes.

Transitions along the x- and y- axes can also be described as electronic oscillations (18). This theory very much depends on the axes of the molecule being different in terms of the structure (19, 20). This theory seems to hold for dyes such as malachite green and methylene blue (19) and Victoria blue dyes (20). The main absorption band in this theory occurs due to transitions along the x-axis and it depends solely on the fraction of characteristic charge that is on the auxochromes (19).

Unfortunately, this theory cannot be applied to dyes which are more symmetrical e.g. crystal violet, as the transitions along the x- and y-axes would be the same. Therefore, this theory would have predicted that symmetrical dyes would only have one absorbance band present. This is not the case for the dye crystal violet as it still has two absorbance bands present in the spectrum.

Another theory found is that triarylmethane dyes exist as isomers. Initial literature articles focussed on the dyes crystal violet and malachite green for this theory, the primary focus was on crystal violet (21). The first conclusions found to be made were that two stereo-isomers were present, one labelled as A, which was a symmetrical helical type and another labelled B, a distorted helical type (21). Subsequently, more papers have emerged trying to prove the isomer theory. An article on spectral bleaching of crystal violet, determined that 2 ground state isomers existed in equilibrium (22). The ground state isomers where deemed to be solvation isomers. The solvation isomers are noted to have a D_3 or C_3 symmetry (22).

Others state that rotational isomers cause the second absorbance band (23, 24). One of the articles determined this through the use of two Gaussian peaks, which were fitted using a least squares curve-fitting method (23). The other paper noted that increasing the pressure had an effect on the position of the absorbance bands and that they were redshifted (24).Articles that attributed that secondary absorption peak to isomers, looked mainly at the dye crystal violet. It should be noted for non-symmetrical dyes like Victoria blue R, that there is a difference between the energy transitions S_0-S_1 and S_0-S_2. These energy transitions were dependant on the number of amino groups present (1).

Dye aggregation is where the dye can self-associate. It is suggested that the dyes are able to form dimers and trimers (25, 26). The force behind aggregation occurring was assumed to be the hydrophobic interaction of dimethylamino groups (26). However, aggregation as a theory is limited as it cannot be applied to all triarlymethane dyes. A study of malachite green found that dimerization did not occur (26). The theory of aggregation is able to link to symmetry considerations, as the aggregation would alter the original symmetry operations present in the molecule.

Ion-pairing is different from aggregation as it involves the interactions between the solute and the solvent. The shoulder peak seen on the absorbance spectra of the triarlymethane dyes was attributed to a solvated ion of the dye in a polar solvent (3, 17, 27). This ability to be solvated was very much dependant on the

environment in which the dye was placed (17, 27, 28). However, it was found that when the solvent was water and the concentration was increased, ion-pairing as a theory broke down. This was linked to aggregation being the cause (3). The conclusion drawn was that as the concentration of the triarylmethane dye solutions was increased, the resultant absorbance spectra would differ by a third absorbance band being present (29).

It is notable that ion-pairing theory focuses very much in the solvent used, and the solvent is thought to interact with the central carbon atom of the dye structure (28). This hypothesis of this structure is backed up by kinetic studies, where a colourless carbinol is the resultant product of the reaction between the dye and hydroxide ions (30). It is seen on the spectrum that micro-solvation causes a red-shift and broadens the peaks (28). Micro-solvation is where a single solvent molecules surrounds a solute molecule (28). To achieve micro-solvation theoretical calculations are done as well as studying the photodissociation spectrum (28).

Theories involving symmetry focus on the molecular shape of the dye. Initially the dyes used in this investigation are found to have a planar shape, though this shape can change due to steric effects in solution, causing lowering of the symmetry order (31). The changes in symmetry of the dyes, could separate degenerate orbitals therefore allowing for more transitions to occur (32). The now distinguishable orbital gives rise to the secondary absorbance peak (32). The secondary absorbance peak corresponds to a band of higher frequency (31).

A large number of articles have been published regarding changes in symmetry causing a secondary peak to occur on triarylmethane dye absorbance spectra (33-39) and not the existence of isomers. However, this has its own limitations as asymmetric dyes in the triarylmethane dye class (like rosaniline), increase the number of isometric forms present therefore re-introducing the isomer theory (16).

The symmetry of the crystal violet in solution was found in the literature to be a D_3 propeller form (34, 35). Ways of describing the symmetry change in solution have been described as torsional twisting (37), or bond rotation and restoration of electronic symmetry (38). Further information found within the symmetry theory is that the π electrons from the phenyl ring where not involved in the x-band transitions, though the change in symmetry made available the π -π* orbital transition for the y-band (38). Changes in symmetry could also be induced by altering the auxochrome, to cause asymmetry thus resulting in a second absorbance band (33).

The environment in which the dye can be found was deemed to have a profound effect on the absorbance spectra. Information regarding how the solvent exactly interacts with the dye molecule is not available. The suggested interaction between the solvent and the central carbon atom on the dye is thought to broaden the peak on the absorbance spectrum (28). This is backed up by kinetic studies carried out on the dye class (30).

Some solvents can have a very visible effect on the colour of the dyes. For example, crystal violet in acidic solvent changes the colour by going into the yellow part of the visible spectrum (16). This is due to the formation of quinoid structures of the dye in the acidic solvent (16).

With focus on the alcohol solvents, an article deemed that the increase in chain length of the solvent, cause's bathochromic shifts (red-shifts of the absorbance peak) (40). Triply substituted dyes like crystal violet, exhibit sensitivity to the solvent dielectric constant, which is taken as a measure of the solvent's polarity (40).

Temperature effects on the absorbance spectra have been linked to the solvent as well. It is seen that decreasing the temperature decreased the "shoulder" (1, 17, 22, 34). The explanation as to why only one peak was present at low temperatures, was related to how the solvation changes with temperature (17). Another way of explaining this is that at low temperatures the main absorption peak was due to isolated molecules in a solvent cavity (1). Contrary to this, crystal violet in acetone and toluene produced absorbance spectra that were independent of temperature (34).

Aims and Objectives

Drawing upon the strands of research that has already been conducted, this study attempts to explain the triarlymethane dye absorbance spectra with regards to temperature and solvent effects and linking this to the theories that have been explained in this introduction. To achieve this, the following aim and objectives were set for this study.

The aim of the study was to validate the theories behind the shoulder present on the absorbance spectra of triarlymethane dyes.

In order to complete the aim, the following objectives were set:

1) To manipulate the shoulder that is present on triarlymethane dye absorbance spectra.
2) To determine how/if symmetry plays a role in the presence of the shoulder.
3) To use the results from 1 and 2 to determine which of the theories holds more precedence.

Methodology

Reagents

The dyes were used as supplied from the manufacturer, no purification was undertaken. Three of the dyes, ethyl violet, brilliant green, and Victoria blue R were purchased from Sigma Aldrich. Crystal violet and malachite green were obtained from Acros Organics.
Five solvents were used, these were: Milli-Q water, methanol, ethanol, propan-1-ol, butan-1-ol. The methanol, and ethanol were HPLC grade supplied by

Fisher. The propan-1-ol was also supplied by Fisher though it was analytical grade. The butan-1-ol was glass distilled grade and supplied by Rathburn Chemicals. Milli-Q water was produced using a Millipore system to a resistivity of 18 MΩ cm.

Solutions

Stock solutions of the dyes to be dissolved in each solvent were made by weighing out the amounts in Table 1, on a calibrated analytical balance in 25 mL beakers.

Table 1: Mass of dye used to make up each stock solution.

	Crystal violet	Ethyl violet	Malachite green	Brilliant green	Victoria blue R
Solvent	Amount of dye weighed out (g)				
Milli-q water	0.03980	0.04935	0.09290	0.04820	0.04510
Methanol	0.04090	0.05070	0.09360	0.04810	0.04530
Ethanol	0.04030	0.04867	0.09092	0.04813	0.04539
Propan-1-ol	0.04100	0.04921	0.09127	0.04857	0.04585
Butan-1-ol	0.04036	0.04957	0.09173	0.04861	0.04482

The amounts in Table 1, were dissolved in a small amount of the solvent and transferred into 100 mL volumetric flask. The 25 mL beaker was washed 3 times with the solvent and all washings were transferred into the volumetric flask. The volumetric flask was then filled to the 100 mL mark using the appropriate solvent.

The final concentrations of the dye stock solutions were approximately 1×10^{-3} M and these stock solutions were stored in 125 mL plastic bottles in the dark.

The stock solutions were diluted to 1×10^{-5} M before absorbance spectra were taken. To do this, a calibrated Rainin Classic air-displacement pipette was used to take 100 μL of the stock solution and transfer into a 10 mL volumetric flask. The volumetric flask was filled to the 10 mL using the appropriate solvent.

Absorbance spectra at room temperature

Absorbance spectra of the dyes where taken at room temperature on Hewlett Packard 8435 photodiode array spectrometer. The instrument was set to produce a spectrum for the wavelength range 350-800 nm. Room temperature was measured using a thermometer and found to be approximately 22°C.

Initially, a blank was run in the instrument. This was done by filling a glass cuvette with a 1 cm path length with the appropriate solvent. The cuvette was filled to be at least 2/3 full. The cuvette was placed in the instrument and locked in place, for a spectrum to blank the instrument to be taken.

Once the instrument was zeroed, the solvent was emptied from the cuvette. The cuvette was rinsed with the sample, before the cuvette was filled with sample and placed in the instrument. A spectrum was then taken of the sample.

This process was repeated for all dye samples dissolved in the appropriate solvents.

Absorbance spectra at other temperatures

Using dye solutions at the concentration 1 x 10^{-5} M, made in 10 mL volumetric flasks as above. Four temperature ranges were selected to study absorbance spectra of the dyes. These are found in Table 2.

Table 2: Temperature ranges for absorbance spectra to be produced at.

	Temperature ranges (°C)
1	50-40
2	40-30
3	20-10
4	10-0

To produce absorbance spectra between the temperature ranges in Table 2, an ice bath and water bath were used to heat and cool the sample to between the highest and lowest temperature ranges.

Using the diode array instrument as before an appropriate blank was initially run. A cuvette filled 2/3 full of the hot or cold dye solution was place in instrument, a thermocouple (Comark 2001) was then placed in the cuvette. The thermocouple was used to obtain the temperature of the solution before and after the absorbance scan. The thermocouple had to be removed from the solution during the absorbance scan in order not to block the light path.

The sample was then warmed or cooled further to the next temperature range (Table 2), before producing the next absorbance scan and obtaining the temperature values before and after that scan.

Precision experiment

Two experiments were performed to assess the precision and help to quantify the uncertainty. These two experiments were performed on the dyes crystal violet and malachite green both dissolved in Milli-Q.

The first experiment for the precision work, involved preparing a solution of the dye to the same concentration as previous work undertaken of 1 x 10^{-5} M. The instrument was blanked using Milli-Q water and following this the cuvette filled 2/3 full of the solution and placed in the instrument. When the cuvette was in the instrument 10 consecutive absorbance scans were taken on the same

solutions. This experiment will be referred to as precision experiment one throughout this report.

The second experiment to be carried which will be referred to as precision experiment two, involved the preparation of 5 solutions. These were made by diluting the stock solution to a final concentration of 1 x 10^{-5} M. After the initial blank of the instrument was performed, each solution was poured into the same cuvette ahead of producing the absorbance spectrum.

All values obtained were used to assess the uncertainty which is further described in the precision section.

Analysis of results

To obtain the secondary peak value, first order derivative spectra were produced. The secondary peak value was then obtained by half the distance between the two inflection points as identified in Figure 2.

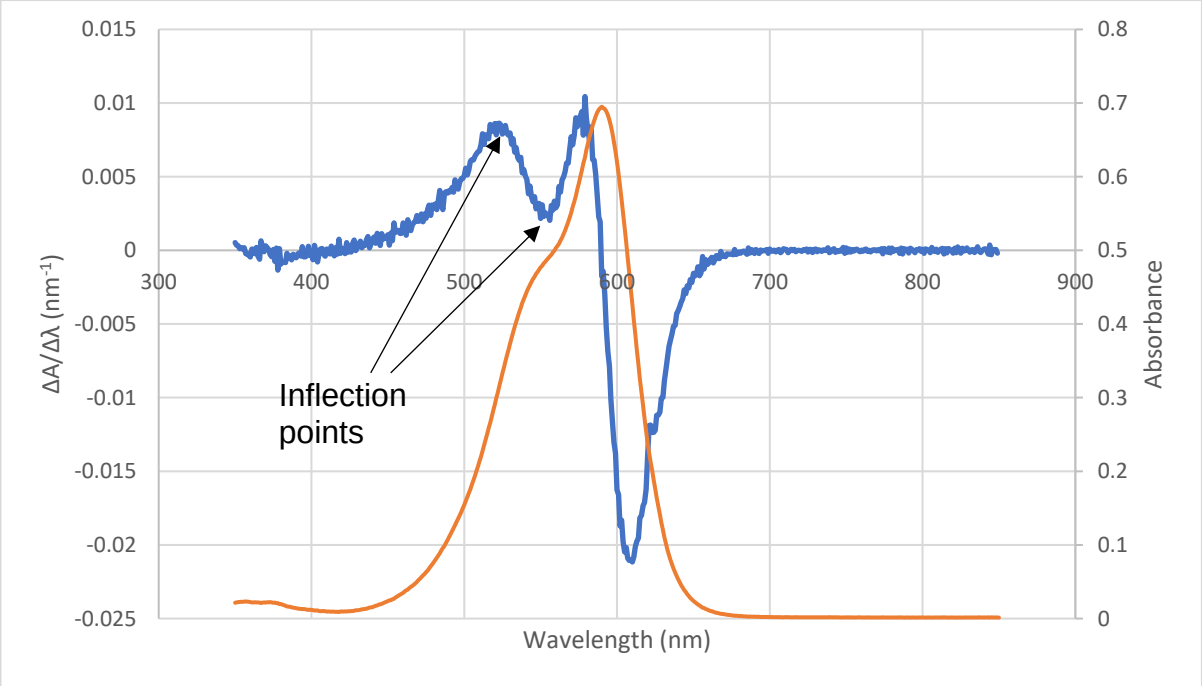

Figure 2: Blue line, the first derivative spectrum, orange line is the absorbance spectrum, of crystal violet in Milli-Q, 10 µM, at room temperature with inflection points labelled.

The reason behind obtaining the first derivative spectrum as shown in Figure 2, rather than use deconvolution software is because deconvolution software can produce conflicting results, even when using the same algorithm (3).

The parameter Δv, was calculated by converting the wavelength values for the major and secondary peak to wavenumbers. The following equation then could be applied:

$$\Delta\nu = shoulder\ value - major\ peak\ value$$

The degree of separation could then be analysed against the solvatochromic parameters for each solvent. The separation parameter $\Delta\nu$, is an approximate parameter rather than a precise difference in energy (3).

Also, from the absorbance spectra obtained, the extinction coefficients were calculated for each of the λ_{max} values. The λ_{max} value was taken from the absorbance spectra produced as the peak with the highest intensity or the longest wavelength value. This was done using the following equation:

$$A = \varepsilon cl$$

Where A is the absorbance value taken from the spectra, c is the concentration of the solution, 1 x 10^{-5} M, and l is the path length, 1 cm.

The dye structures were analysed by group theory. Group theory allows for mathematical interpretation of the symmetry elements displayed within a molecule.

Results and Discussion

Purity of dyes

Initially, purification was attempted by recrystallisation of the dyes in methanol. The recrystallisation was performed on the crystal violet dye, the first attempt used 5 g of dye and the second time the procedure was undertaken using 1 g of dye. Both times no crystals were obtained. It was noted that due to the intense colour produced by the dye if crystals were present they were difficult to distinguish.

Although from literature recrystallisation of the dyes should have yielded some results, and an article stated that recrystallisation in methanol worked (1), the inconsistency, may be the result of lack of information being available. This is because journals tend not to publish full and detailed methods of the experiments undertaken.

Only two attempts at recrystallisation were undertaken due to time constraints, to not take away from the scope of the project and since literature provides in consistent approaches on purifying these dyes.

From further research, other methods of purification were identified. These included, but were not limited to; dialysis and electrodialysis and precipitation by sodium acetate (41). For basic dyes, recrystallisation may be done in different solvents, this includes water-ethanol mixtures and dilute hydrochloric acid. However, to achieve maximum purity, three recrystallisations are required. Dialysis and electrodialysis are methods that are mainly of theoretical interest. They have many disadvantages, including the long time required to undertake it, the membranes are difficult to prepare and only low purity is

achieved. Considered one of the best methods for purifying dyes is, precipitation by sodium acetate. The method is widely applicable to the vast range of dyes available and yields high purity results (41). However, the method does have its disadvantages, dyes which are alcohol soluble will yield low results, it is tedious and involves filtration of colloidal precipitates (41).

Assaying a dye will help determine what impurities are present and then give an idea on the purity of the dye. One way is to do spectrophotometric assay, this requires the determination of the absorbance at the absorbance maximum (42). However, this method of assaying only works if the molar extinction coefficient is known (42). Another limitation of this assay method is that the molar absorbance of many dyes are not available, or are unreliable as the dye may not have been adequately purified (42). Other methods of assaying the dye use chromatography techniques, this includes high performance liquid chromatography (HPLC) and thin layer chromatography (TLC) (42).

The impurities present in a dye sample can vary greatly, though the impurities can be grouped into different categories. The wrong dye present, is more a labelling issue, this is where the dye that is named on the label is not present at all within the sample (42). The dye sample here will be made up of other dyes. The next group is where additional dyes are present (42). This can occur from the synthesis process of the dye.

Finally, impurities can be present as colourless materials. Common colourless impurities are found to be dextrin ad sodium chloride as these as generally introduced in the manufacturing process (42). For brilliant green, the manufacturing process involves condensing one mole of benzaldehyde with diethylaniline, in the presence of either hydrochloric or sulfuric acid (43). This process forms the dye in its leuco form, this is then oxidized and converted to the acid sulfate (43).

Spectrophotometric Assay

As previously mentioned a spectrophotometric assay can be obtained by comparing an extinction coefficient with that in literature. By completing a photometric assay of the dyes, a comparison can be made for the dyes which the manufacture provides a purity value for.

The spectrophotometric assay, has been done on ethyl violet in methanol. Figure 3, shows the absorbance spectrum for ethyl violet.

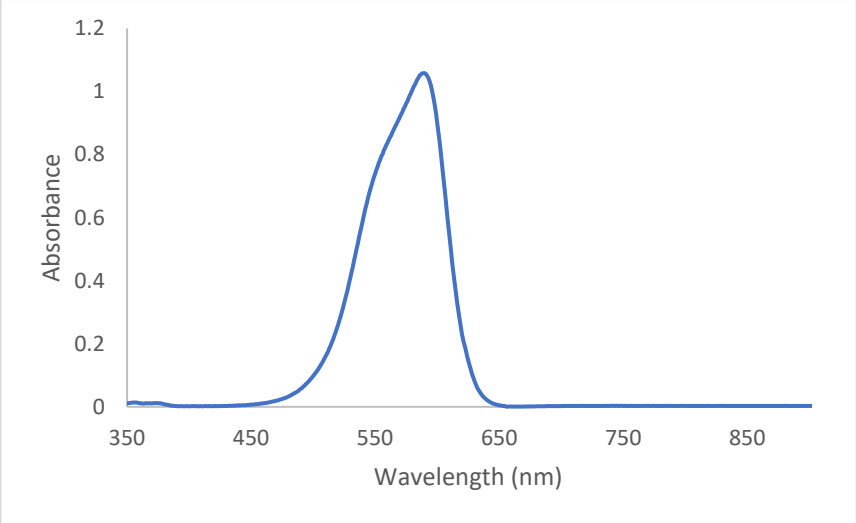

Figure 3: Absorbance spectrum of ethyl violet in methanol at 1 x 10^{-5} M.

From Figure 3, absorbance value for the λ_{max} the extinction coefficient can be determined. This was found to be 10, 5810 L mol^{-1} cm^{-1}. The paper by Lewis et al., published the extinction coefficients they found. For ethyl violet in methanol, they published a result of 10, 6000 L mol^{-1} cm^{-1} (1).

By comparing the two values using the follow equations allows for a percentage purity to be found:

$$percentage\ purity\ = \frac{experimental\ value}{Literature\ value}\ x\ 100$$

This found that the percentage purity for ethyl violet is 99.8%.

To further ensure that this percentage purity found was indeed correct a further spectrophotometric assay was done this time, using ethyl violet in ethanol (Figure 4).

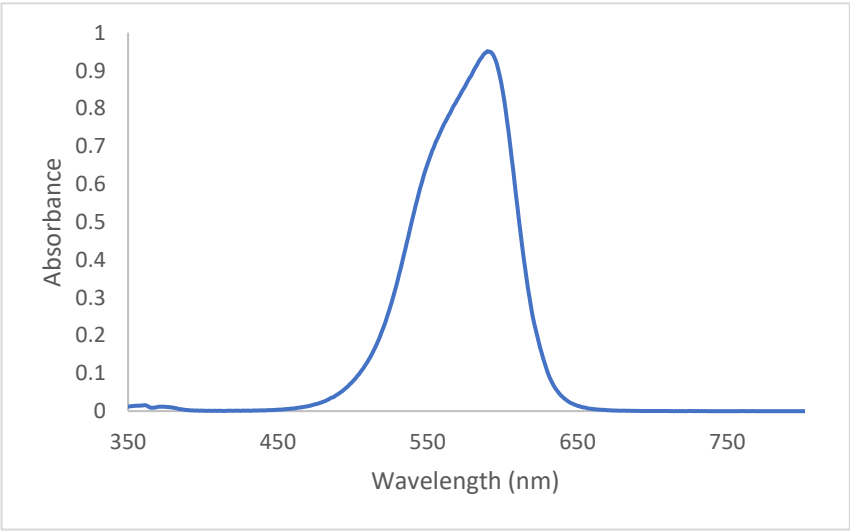

Figure 4: Absorbance spectrum of ethyl violet in ethanol.

Extinction coefficient found from the Figure 4, was 95134 L mol^{-1} cm^{-1}. The literature found a value of 10, 1000 L mol^{-1} cm^{-1} (1). Therefore, the percentage purity this time was determined to be 94.2 %.

The manufacturer has a quoted value, of greater than 90% (44). The two percentage purity values seem to be in accordance with what the manufacturer stated. Therefore, it can be interpreted that all dyes are of a high purity and in-line with the manufactures purity value for them.

Symmetry

The second objective set for this dissertation was to determine how/if symmetry plays a role in the electronic transitions. To achieve this the symmetry operations and properties were analysed by a branch of mathematics called group theory.

As mentioned in the literature review, the cause of the secondary peaks had been noted to do with the symmetry of the molecule. Firstly, the symmetry operations of the 5 dyes were determined. The symmetry operations are related to the shape of the molecule, here 3 shapes were analysed for each dye. The shapes are planar, propeller and twisted propeller. These shapes were selected due to being referenced throughout relevant literature.
It is necessary here to clarify exactly each of the symmetry operations symbols mean.

E, is the identity operation or more commonly expressed as the molecule's original starting position.

C_n, this is the rotation around an axis of symmetry. The C stands for proper rotation and the n denotes the order to which the degree of rotation occurs. Therefore, a C_2 symmetry operation is a proper rotation which is rotated by half a turn along an axis. A C_3 operation, again is a proper rotation though this time the rotation is by 1/3 of a turn rather than a half, a long a certain axis.

The next two symmetry operations to be described are reflections in the planes of the molecule. σ_h, is the reflection in the plane that is perpendicular to the principal axis of the molecule. The h denotes that this is horizontal. Therefore σ_v, is the reflection in the plane which contains the principal axis. The v denotes that this vertical. Both σ_h and σ_v, can be expressed as mirror planes of symmetry.

The symmetry operations present in a molecule can then be placed into point groups. These point groups show all the symmetry operations present in the molecule rather they identify key symmetry operations that are present (45, 46).

Planar shape

Initially the dyes were analysed in the planar shape, Figures 5-7 show the structure of the dyes in the planar shape.

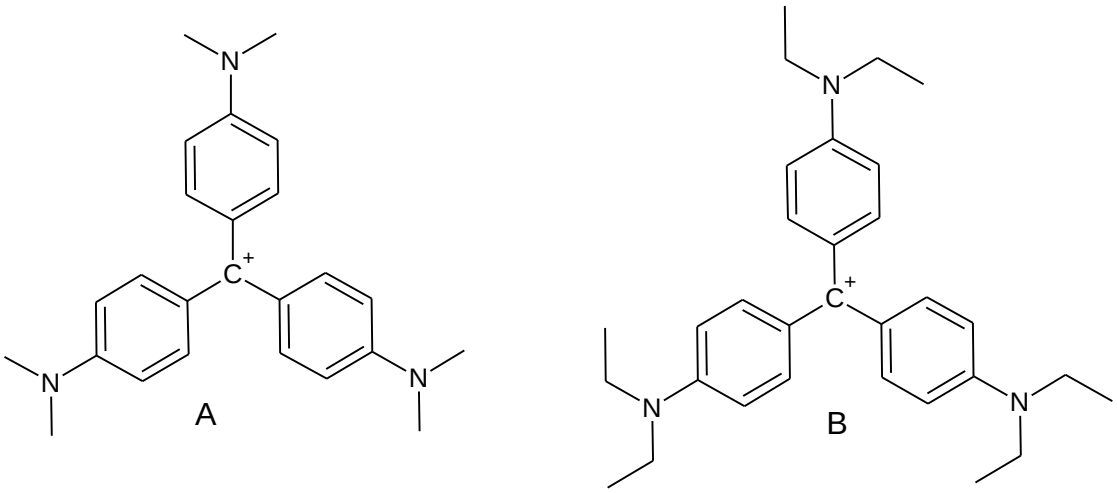

Figure 5: Structures of A- crystal violet and B- ethyl violet.

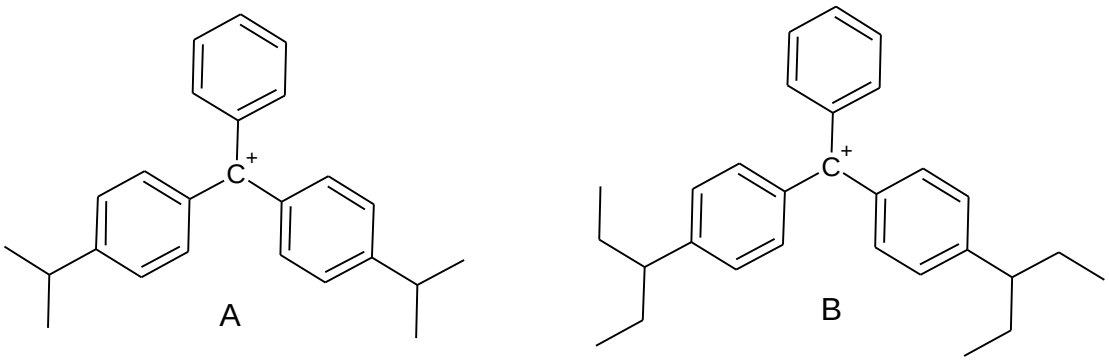

Figure 6: Structures of A- malachite green and B- brilliant green.

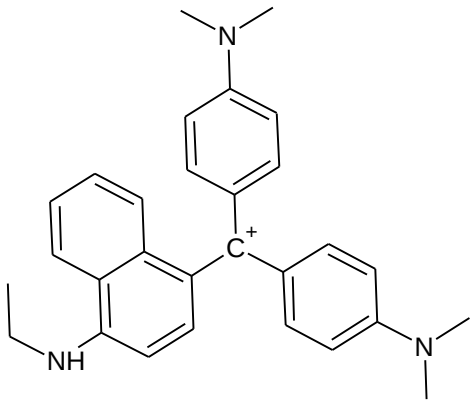

Figure 7: Structure of Victoria blue R dye.

Table 3: lists the symmetry operations present for each dye and gives the relevant point groups for the planar shape.

Table 3: Point groups and symmetry operations of dyes in the planar shape.

Dye	Point Group	Symmetry operations present in a planar shape.
Crystal violet	D_{3h}	E, C_3, σ_h, $3\sigma_v$, $3C_2$
Ethyl violet	D_{3h}	E, C_3, σ_h, $3\sigma_v$, $3C_2$
Malachite green	C_{2v}	E, σ_v, C_2
Brilliant green	C_{2v}	E, σ_v, C_2
Victoria Blue R	C_s	E, σ_h

From an initial glance at Table 3, it shows that the number of symmetry operations decreases as you go down the table from crystal violet to Victoria blue R. Both crystal violet and ethyl violet have the same symmetry operations. This is due the structures in Figure 5 only differing by the side chains. This is the same for malachite green and brilliant green in Figure 6, where their side chains differ only by the number of carbons present.

Propeller shape

The propeller shape of the dyes can be described as all the benzene rings being rotated in the same direction. Here the 3D models for crystal violet (Figure 9) and malachite green (Figure 8) show the rotation of benzene rings, as seen from an angle where to look through the molecule.

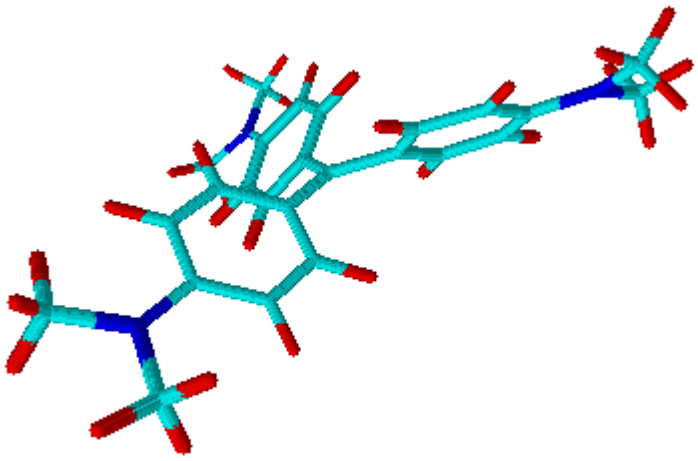

Figure 8: 3D optimised model of crystal violet in a propeller shape.

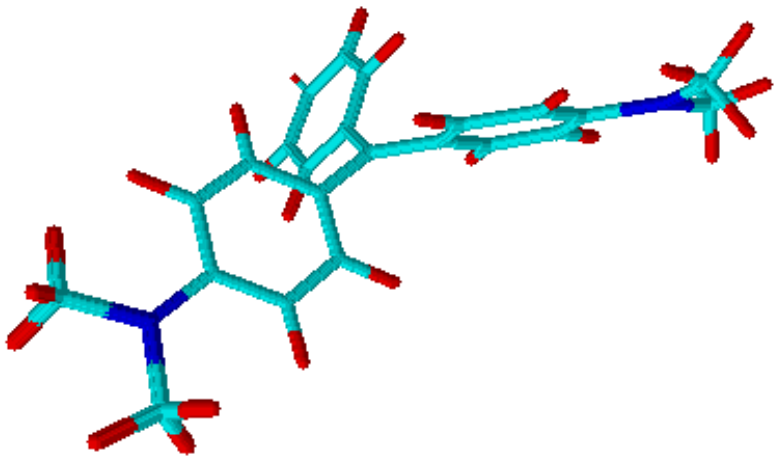

Figure 9: 3D optimised model of malachite green in a propeller shape.

In Figures 8 and 9, the red shows the hydrogens, the light blue represents the carbon atoms and the dark blue represents the nitrogen atoms. The symmetry and point groups of the propeller shape dyes are found in Table 4.

Table 4: Point group and symmetry operations present of dyes in the propeller shape.

Dye	Point group	Symmetry operations
Crystal violet	D_3	E, C_3, $3C_2$
Ethyl violet	D_3	E, C_3, $3C_2$
Malachite green	C_2	E, C_2
Brilliant green	C_2	E, C_2
Victoria blue R	C_1	E

As with Table 3, there is a decrease in the symmetry operations present going down Table 4, from crystal violet to malachite green. From the planar shapes in Table 3, there are more symmetry operations present compared to the propeller shapes. The propeller shape for the dyes does alleviate some of the steric effects that are seen due to the hydrogens on the benzene rings.
All dyes in the propeller shape lose the planes of symmetry that were present in the planar shape.

Twisted propeller shape
The twisted propeller shape is similar to that of the propeller shape. Though, the only difference being that one of the benzene rings is twisted in the opposite direction to the others. This shape allows for two-point groups to be available for malachite green and brilliant green, as it depends on whether the substituted or un-substituted benzene ring is twisted in the opposite direction. Table 5, shows the point groups for the dyes in this twisted propeller shape.

Table 5: Point group and symmetry operations present of dyes in a twisted propeller shape.

Dye	Point group	Symmetry operations
Crystal violet	C_2	E, C_2
Ethyl violet	C_2	E, C_2
Malachite green – unsubstituted ring twisted oppositely.	C_2	E, C_2
Malachite green – substituted ring twisted oppositely	C_1	E
Brilliant green - unsubstituted ring twisted oppositely	C_2	E, C_2
Brilliant green - substituted ring twisted oppositely	C_1	E
Victoria blue R	C_1	E

Though the symmetry operations have changed from Table 4 for some dyes, the dyes malachite green and brilliant green for the unsubstituted ring twisted and Victoria blue R there is no change in the symmetry operations. The substituted ring twisted in malachite green and brilliant green have a C_1 point group. This is a special kind of symmetry where only the identity, E is present, this is the same for Victoria blue R.

There is a relationship between electronic transitions and symmetry. As previously stated, for a compound to exhibit a colour, the compound must be capable of being promoted to an excited state. For an electron to be promoted to a higher energy level, causing the molecule to enter an excited state, the transition has to be available.

However, some transitions are unavailable as they are symmetry-forbidden (46). It is concluded that the higher the order of symmetry of a molecule, the higher the probability an electronic transition is forbidden (46). Therefore, applying this statement to the dyes, the planar shapes have the highest probability that some electronic transitions are forbidden. Crystal violet and ethyl violet have the highest symmetry, therefore have the highest probability that electronic transitions are forbidden. The probability that the transitions are forbidden by symmetry decreases as the shape is changed from planar to propeller and then to the twisted propeller form.

Precision

The precision was determined by carrying out two experiments as detailed in the methodology section. Both experiments were done on crystal violet dissolved in Milli-Q and malachite green dissolved in Milli-Q. These two dyes were used to address a best case defined shoulder, with good absorbance and

a shoulder which was present but not as well defined with weak absorbance. The best-case dye was crystal violet and the worst case was malachite green.

Precision experiment 1
As outlined in the methodology section, the first experiment involved taking 10 absorbance scans of the dye solution in the cuvette. This was done to study any changes in wavelength caused by the instrument. The results for both dyes are in Table 6.

Table 6: Precision experiment results for the dyes crystal violet and malachite green.

	Crystal violet		Malachite green	
Scan No.	λ_{max} (nm)	Shoulder wavelength (nm)	λ_{max} (nm)	Shoulder wavelength (nm)
1	591.0	541.0	617.0	571.0
2	591.0	541.0	617.0	571.0
3	591.0	540.0	617.0	572.0
4	591.0	541.0	617.0	572.0
5	591.0	541.0	617.0	570.0
6	591.0	542.0	617.0	572.0
7	591.0	542.0	617.0	571.0
8	591.0	540.0	617.0	572.0
9	591.0	541.0	617.0	570.0
10	591.0	541.0	618.0	570.0
Average	591.0	541.0	617.1	571.1
Standard deviation	0.00	0.667	0.316	0.876

It can be seen from the data in Table 6 that the dye crystal violet had a better standard deviation compared to that found for malachite green. It is noticeable for both dyes from Table 6, that the standard deviation is higher for the shoulder wavelength values than for the main absorbance. The instrument is able to determine the λ_{max} and the value was confirmed in the first derivative spectrum, though the shoulder value was solely determined from the first derivative spectrum.

From this the uncertainty values of $\pm$ 0.3 nm and $\pm$ 0.9 nm for the λ_{max} and shoulder wavelength values respectively, have been applied across all dyes to account for all uncertainties that are present.

Precision experiment 2
Details of how this experiment was conducted can be found in the methodology section. The focus for this experiment was to determine the uncertainty that occurred with regards to making the solution and from the dilution step, where uncertainty is introduced by the pipette and filling to the mark of the volumetric flask. This uncertainty would be reflected in the concentration and therefore would be present also within the absorbance value determined by the

instrument. Table 7, provides the experimental data for the 5 solutions which includes their λ_{max} and the corresponding absorbance value.

Table 7: Precision experiment two, results for crystal violet and malachite green.

	Crystal violet		Malachite green	
Solution Number	λ_{max} (nm)	Absorbance	λ_{max} (nm)	Absorbance
1	591.0	0.65423	618.0	1.013411
2	591.0	0.70875	618.0	1.160805
3	591.0	0.65335	617.0	1.056432
4	590.0	0.63051	618.0	1.488334
5	591.0	0.79314	618.0	1.142924
Average	590.8	0.68799	617.8	1.172381
Standard deviation	0.447	0.0654	0.447	0.187

As before with the first precision experiment, this experiment shows that the malachite green has the higher uncertainty value associated with it. The uncertainty value for the wavelength here maybe reduced upon running more samples and determining the wavelength value. Focussing on the absorbance values (Table 7) which in this case reflect more on the uncertainty from the preparation rather than the instrument, shows that a highest uncertainty value of ± 0.187. Since both the instrument and sample preparation will contribute to the uncertainty of the absorbance the two uncertainties must be combined. This compares to the wavelength values, where only the instrument parameters will affect the value (47). The following equation was used to combine the uncertainties (48):

$$U = \sqrt{u_{\lambda max}^2 + u_{secondary}^2}$$

The combined uncertainty for the absorbance was found to be ± 0.187003, which will be rounded to ± 0.187. This value shows that predominately the uncertainty is lying within the sample preparation rather than the instrument.

Uncertainty Budget

Identification and quantification of all the sources of uncertainty within the experiments preformed is difficult, especially with quantifying them. Here a general overview is given to the expected sources of uncertainty. To help with this, a cause and effect diagram has been constructed (Figure 10). Cause and effect diagrams, or fish bone diagrams are a simple way of showing where uncertainty can be introduced into a measurement (48).

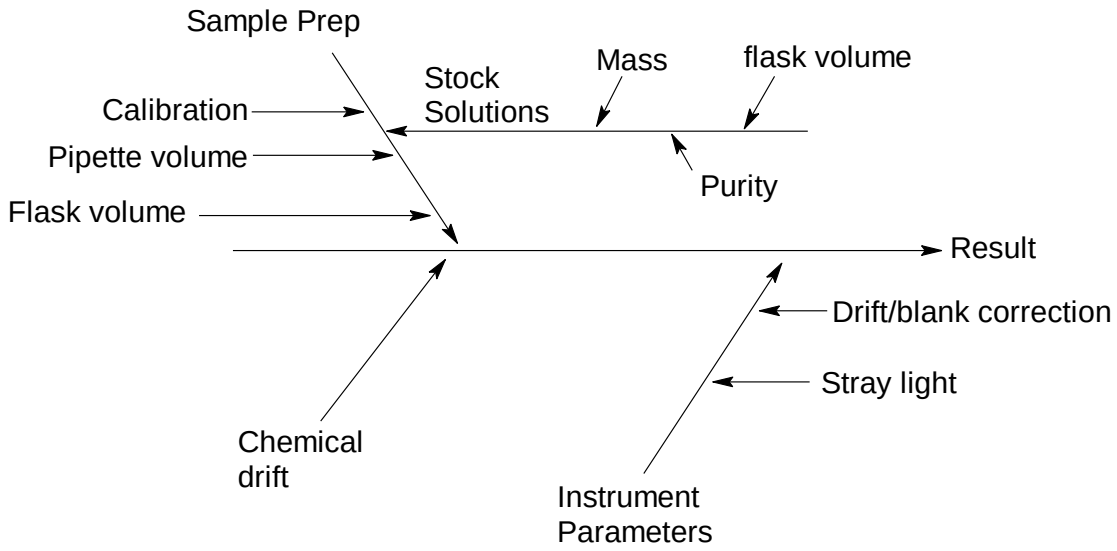

Figure 10: Cause and effect diagram for the uncertainty associated with the absorbance results.

Figure 10, provides an overview of the sources of uncertainty, which have clearly been grouped into sources related to the sample prep and those related to the instrument. The instrumental parameters line (Figure 10) is not an expansive list of all the parameters, instead a couple were selected, to avoid over complicating the diagram.

The top half of Figure 10, is about sample preparation. The sample preparation can be broken down into two parts, the uncertainty surrounding the stock solutions and then the dilution step to produce the final dye solution at a concentration of 1×10^{-5} M. The uncertainty introduced in the stock solution comes from three areas; the mass weighed out, dye purity and flask volume. As previously determined the dye purity was found to be in excess of 90% in accordance with manufacturer's statement.

The volume uncertainty also occurs in the dilution step too, where there is now a volume uncertainty not only associated with the flask but also with the pipette. As previously mentioned the pipetted uncertainty can be reasonably accounted for from experiment 2.

Moving on to focus on the instrument parameter line from Figure 10, it can be found that repeatability uncertainty includes: instrument noise, repeatability of cell position within the cell compartment, any temperature fluctuations, and dust particles on the cell windows or in the solution (49).

Drift can occur within the instrument and this is generally considered to be absorbance drift as drift occurring within the wavelength is minor (49). The absorbance drift can be categorised into two groups:

1) Intrinsic or "physical" drift, this is changes in the spectrophotometer with time
2) Drift caused by changes occurring with time in the solution

The intrinsic drift can be further subdivided into two more groups. These are drift in the base line and drift of the spectrophotometer response (49). The intrinsic drift has been suggested to be dominated by any base line drift (49). Drift though can be accounted for without being included in the uncertainty by normalising the spectra. For this study all spectra were corrected for any base line drift. All instrument parameters as specified by the manufacturer can be found in Tables 8 and 9.

Table 8: Manufacturers specifications for the instrument parameters.

Type	Specification	Comments
Wavelength range	190-1100 nm	
Slit width	1 nm	
Resolution	> 1.6	Toluene in hexane, ratio of absorbances at 269 and 266 nm
Stray light	< 1.0 %	At 200nm, solution of 1.2 % KCl, blank scan on air, 5 s integration time
	< 0.05 %	At 220 nm, solution of 10 g L^{-1} NaI, blank scan on air, 5 s integration time
	< 0.03 %	At 340 nm, solution of 50 g L^{-1} $NaNO_2$, blank scan on air, 5 s integration time
Wavelength accuracy	< ± 0.5 nm	NIST 2034 standard, using transmittance peak minima; wavelength in NIST certificate are interpolated for 1.5 nm bandwidth from the values given for 2 nm and 1 nm bandwidth; uncertainty of standard from NIST certificate (typically ±0.1 nm) is added to the specification; 99-point spline function is used; 0.5 s integration time
Wavelength reproducibility	< ±0.02 nm	Ten consecutive scans with NIST 2034 standard; 0.5 s integration time
Photometric accuracy	< ± 0.005	NIST 930e standard at 1 absorbance, at 440.0, 465.0, 546.1, 590.0 and 635.0 nm, 5 s integration time
Photometric accuracy	< ± 0.001	Potassium dichromate in 0.01 M H_2SO_4 at 235, 257, 313, and 350 nm; blank scan on 0.01 M H_2SO_4, 5 s integration time

Table 9: Manufacturers specifications for the instrument continued.

Type	Specification	Comments
Photometric noise	< 0.0002 rms	Sixty consecutive scans on air with 0.5 s integration time at 0, 500 nm; 11-point moving average: using equation: Noise(rms)=SQRT((SUM(X-x)^2)/n) where x are measured values, X is a 11-point moving average, n is the number of points
Photometric Stability	< 0.001 h^{-1}	Scan on air at 0, 340 nm, after 1-hour warm up, measured over 1 hour, every 60 s, integration time 5 s; difference between maximum and minimum values are compared to specification; at constant ambient temperature
Basline flatness	< 0.001 rms	Scan on air at 0, 340 nm, 0.5 s integration time
Typical scan time	1.5 s	Full range
Shortest time scan	0.1 s	Full range
Time until next scan	0.1 s	Full range, 0.1 s scan, at least 150 consecutive scans

Other instrument parameters which have to be included in the uncertainty budget are the stray light effect. From Table 8 the manufacturer has 3 values ranging from 1.0 – 0.03% for stay light. Table 8 also identifies how these values were produced. The stray light will affect the linearity of the spectrophotometer's absorbance scale (49). This linearity will also be affect by the bandwidth parameter. Stray light is sensitive to the wavelength used and increases with decreasing wavelength value (49). With regards to stray light it has become good practice for accurate quantitative work for the absorbance not to significantly exceed 1.0 (49). As part of good experimental procedure the optics of the instrument should be checked regularly for dust particles as this increases any stray light (49).

Finally, from Figure 10, is the line that introduces any uncertainty due to chemical drift. Chemical drift is the manifestation of changes in absorbance as a result of changes in the solution (49). This change in the solution's absorbance may be caused by the following (49):

1) Reaction of the matrix compounds, resulting in an absorbing species

2) Reactions of the analyte with oxygen
3) Decomposition of analyte

For these dyes, point one of reaction of the matrix compounds, in this case would be the dyes self-associating. This theory known as aggregation previously mentioned in the literature as the cause of the shoulder. Further work has found that malachite green and brilliant green are unable to self-associate (38). Also, even in neutral triarlymethane dyes a shoulder is present and aggregation cannot occur due to lack of charge (50). It has also been suggested in one study that at the low concentration used in this study aggregation is unable to occur (1).

Decomposition of the analyte can result in the creation of two products one being the carbinol and the other being the leuco form of the dye. Both are presented in Figure 11, using crystal violet as the example.

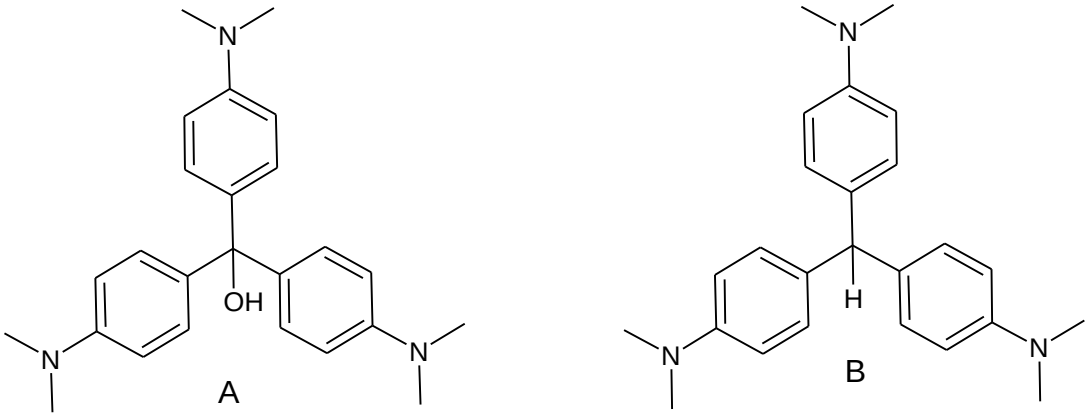

Figure 11: Structure of a) crystal violet carbinol and b) crystal violet leuco form.

Both the carbinol and leuco dye from are colourless, therefore will not absorb and if present in the solution will introduce that uncertainty in the absorbance through the chemical drift.

Even with the advances in instrumentation not all the sources of uncertainty can be quantified (49). This section has explained the uncertainty results produced from carrying out two experiments on two of the dyes. Furthermore, it has explained the sources of uncertainty to be found within the experimental work and importantly UV-vis spectrophotometry.

Solvent Effects

This section focuses on how the solvent influences the absorbance spectrum of the dye and this section considers all the results taken at room temperature, in order to achieve objective one.

Room temperature in this case was found to be approximately 22°C. The solvents studied were 4 alcohols ranging in chain length C_1-C_4, and Milli-Q water. The concentration of all solutions was 1 x 10^{-5} M.

Initially considering the λ_{max} values only in Table 10, these values were obtained for dyes crystal violet, ethyl violet, malachite green and brilliant green to be the wavelength with the highest absorbance value. For Victoria blue R, the absorbance value with the longest wavelength was taken as λ_{max} due to similar intensity values for the 2 peaks.

Table 10: λ_{max} values for the dyes in each solvent.

Dye	$\lambda_{max} \pm 0.3$ (nm)				
	Methanol	Ethanol	Propan-1-ol	Butan-1-ol	Milli-Q water
Crystal violet	587	589	590	590	590
Ethyl violet	590	590	592	592	595
Malachite green	619	622	624	625	617
Brilliant green	626	628	629	630	625
Victoria blue R	617	625	627	627	613

It is apparent from Table 10, that when looking at the alcohol class of solvents alone, which are of chain length C_1-C_4, that there is obvious bathochromic shift trend with the increasing chain length. A bathochromic shift is where the spectral band has been shifted to the longer-wavelength part of the spectrum (red shift) (5).

These results are in accordance with findings by Lewis, et al., (1). Where bathochromic shifts were also observed for the alcohol class of solvents with increasing chain length.

Table 11, shows the dielectric constant and solvatochromic parameters for each solvent. The solvatochromic parameters are all associated with spectral shifts in absorbance bands (51). The parameter, α, is the hydrogen-bond acidity, β is the hydrogen-bond basicity and π* is the polarizability (51).

The dielectric constant, given the symbol ε or ε_r is taken as a measure of a substance's ability to insulate charges from each other. It is also related to the solvent's polarity, this means the higher ε_r value the higher the polarity and the greater ability to stabilize charges. In this work, the symbol ε_r will be used for the dielectric constant so as to not confuse this with the extinction coefficient which also uses the symbol ε.

Table 11: Dielectric constant and solvatochromic parameters α, β and π* for each solvent.

Solvent	Dielectric constant, ε_r (52)	π* (1)	α (1)	β (1)
Methanol	33.0	0.60	0.93	0.62
Ethanol	25.3	0.54	0.83	0.77
Propan-1-ol	20.8	0.52	0.78	-
Butan-1-ol	17.84	0.47	0.79	0.88
Water	80.1	1.09	1.17	0.18

When considering the alcohol class alone, it is noticeable in Table 11 that methanol has the shortest chain length and highest values for dielectric constant and the solvatochromic parameters α and π*, and the lowest value for β. The dielectric constant and solvatochromic parameters, α and π* then decrease in value as chain length of the alcohol increases. The opposite trend is observed for the solvatochromic parameter β which increases in value with increasing chain length. The solvatochromic parameters were obtained from literature (1), though it is unclear as to why propan-1-ol does not have a β parameter value. Note that there is a discrepancy in the trend of α values between propan-1-ol and butan-1-ol, which will be discussed further below.

For the dyes crystal violet, ethyl violet and Victoria blue R only have two absorption peaks in their absorbance spectra in the visible range. This is not the case with brilliant green and malachite green. Figure 12, shows the absorbance spectrum of malachite green in Milli-Q water.

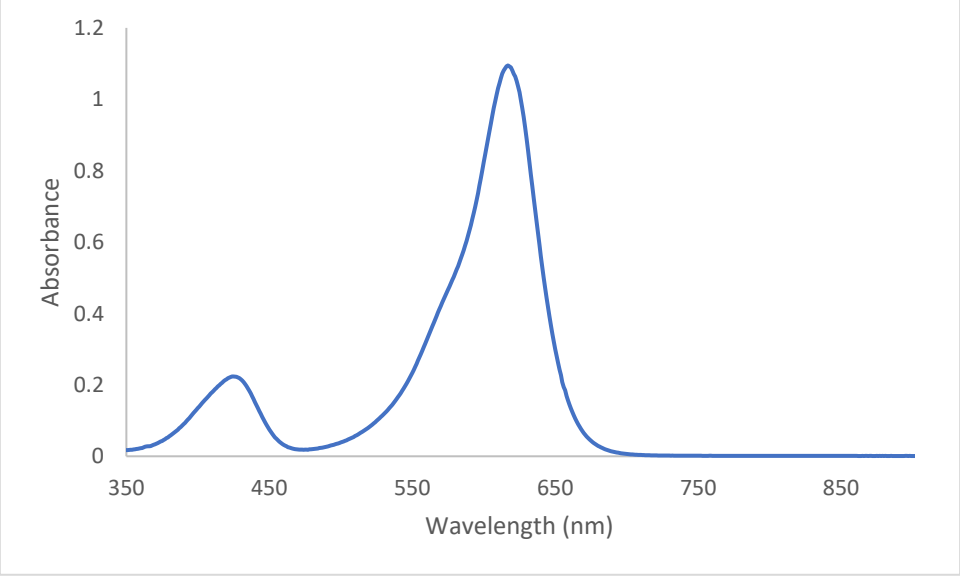

Figure 12: Absorbance spectrum of malachite green in Milli-Q water.

Figure 12 shows that there is a shoulder peak to the main absorption band at 617 nm and a peak at 425 nm. One study identifies the peak at 425 nm, to be

the secondary absorbance peak (33), whilst another study using deconvolution software determined that there were 5 Gaussian curves in the spectra of brilliant green and malachite green (40). For this study, only the relationship of the shoulder peak to the main absorbance band ($\Delta\nu$) has been considered.

Figures 13-17 have been plotted to show the relationship between the dielectric constant and $\Delta\nu$. The degree of splitting $\Delta\nu$, is in wavenumbers to allow for comparison with literature results. On all graphs plotted the combined uncertainty has been calculated and is shown as the error bars, this allows for the obvious trend to be observed. The combined uncertainty was calculated by taking the uncertainty found of ± 0.9 nm for the shoulder value and ± 0.3 nm for the λ_{max}. In order to convert through to wavenumber extreme values were taken each side of the shoulder value and λ_{max}. These extreme values were converted into wavenumbers and the difference found between the extreme value and the λ_{max} or shoulder value. The two differences found were then combined.

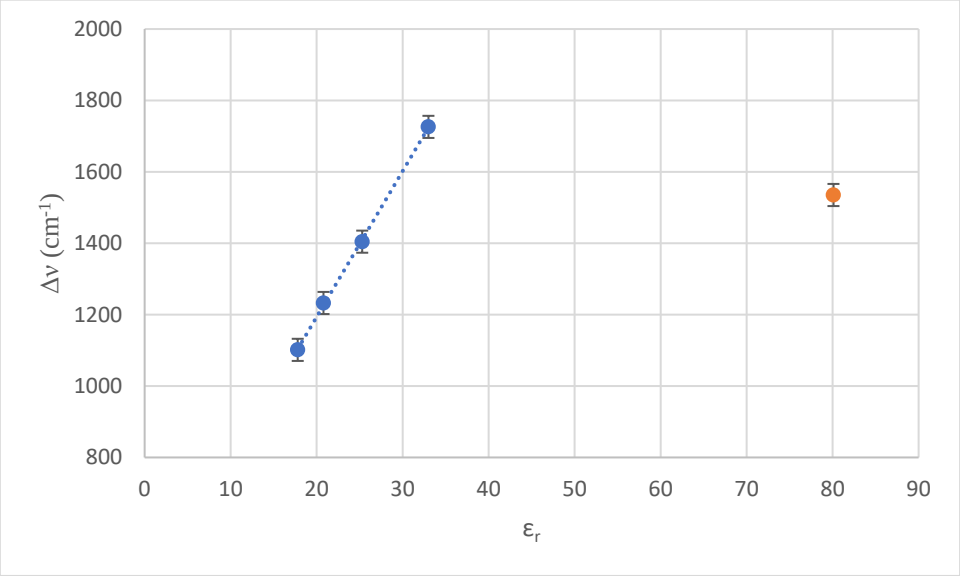

Figure 13:Δv against ε_r for crystal violet, alcohol results in blue and Milli-Q water result in orange.

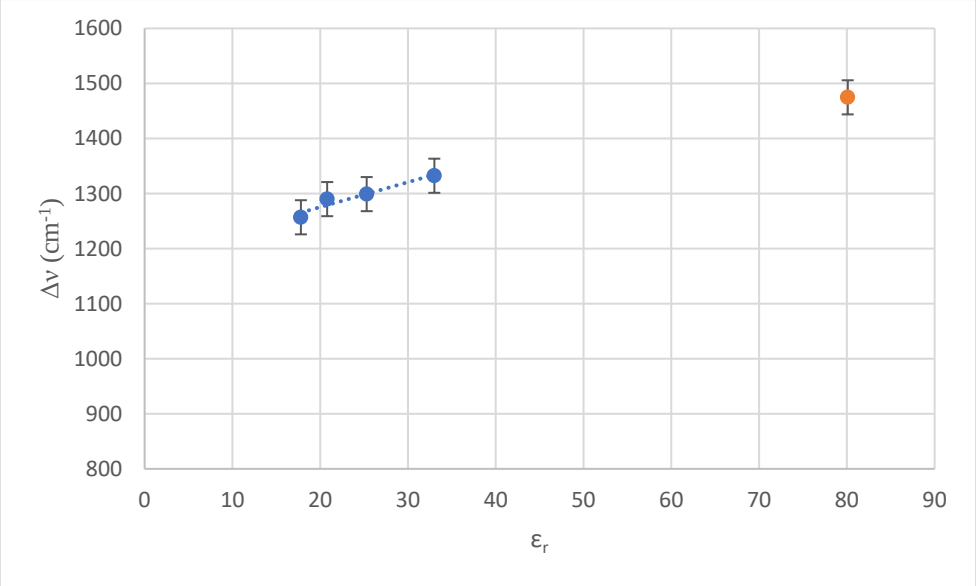

Figure 14: Δν against ε_r for ethyl violet, alcohol results in blue and Milli-Q water result in orange.

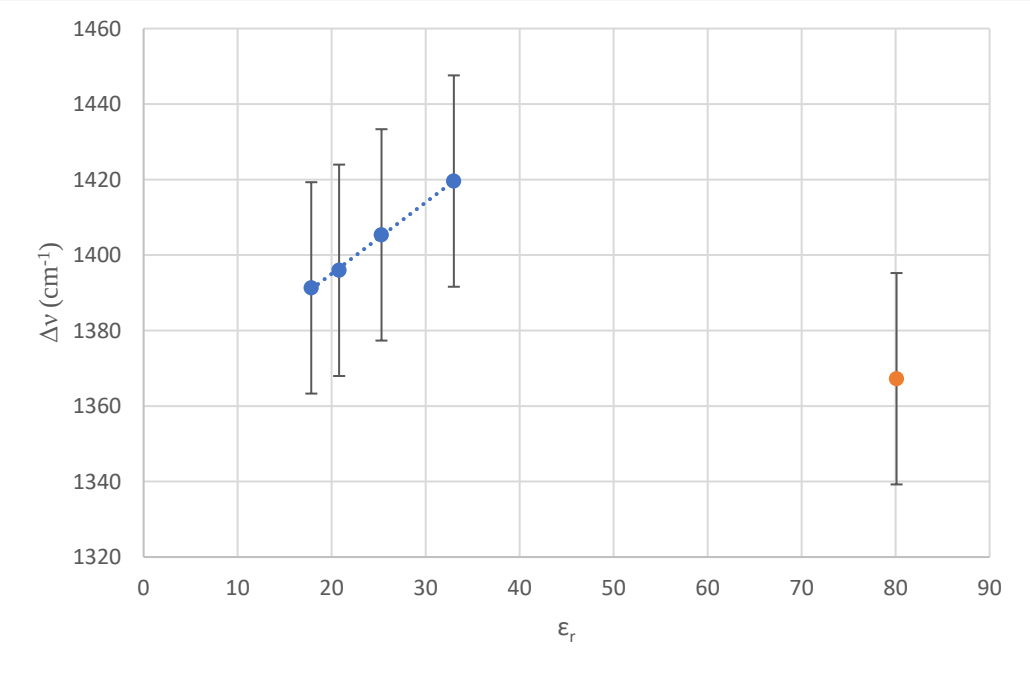

Figure 15:Δν against ε_r for malachite green, alcohol results in blue and Milli-Q water result in orange.

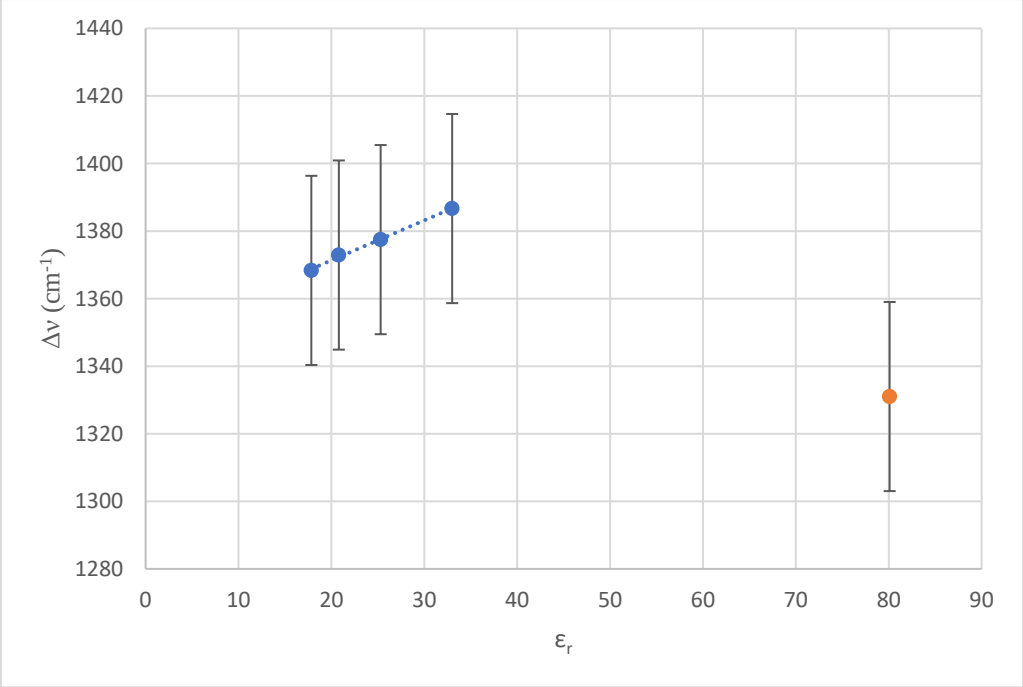

Figure 16: Δν against ε_r for brilliant green, alcohol results in blue and Milli-Q water result in orange.

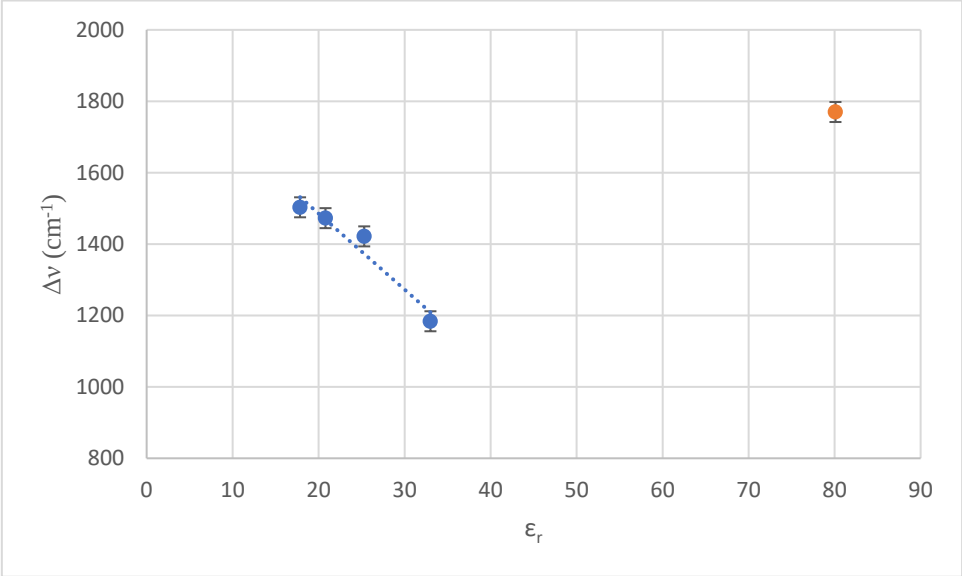

Figure 17: Δν against ε_r for Victoria blue R, alcohol results in blue and Milli-Q water result in orange.

Figures 13-16 reveal that for crystal violet, ethyl violet, malachite green and brilliant green there is a positive linear trend between Δν, and the dielectric constant for the solvent. This is the opposite with Victoria blue R as Figure 17 shows that the trend is linear but Δν decreases with increasing dielectric constant.

Considering only for now Figures 13-16, the increase in $\Delta\nu$ with increasing dielectric constant demonstrates that there is bathochromic shift occurring for the main absorbance band and a hypsochromic shift for the overlapping secondary absorbance band. As methanol has the highest dielectric constant studied for the alcohol solvents, this shows the highest degree of splitting between the two absorbance bands. Previous work has proposed that the main absorption peak is related to a π-π* transition and the secondary peak to a n-π* transition (46). In contrast to this is Victoria blue R, which has $\Delta\nu$ decreasing with increasing dielectric constant. It is unclear as to why the trend is opposite for Victoria blue R.

The relationship between the solvent and the dyes can also be analysed through $\Delta\nu$ and the solvatochromic parameters found in Table 2. Figures 18-22, show the relationship for each dye with the α parameter, this is the hydrogen-bond acidity.

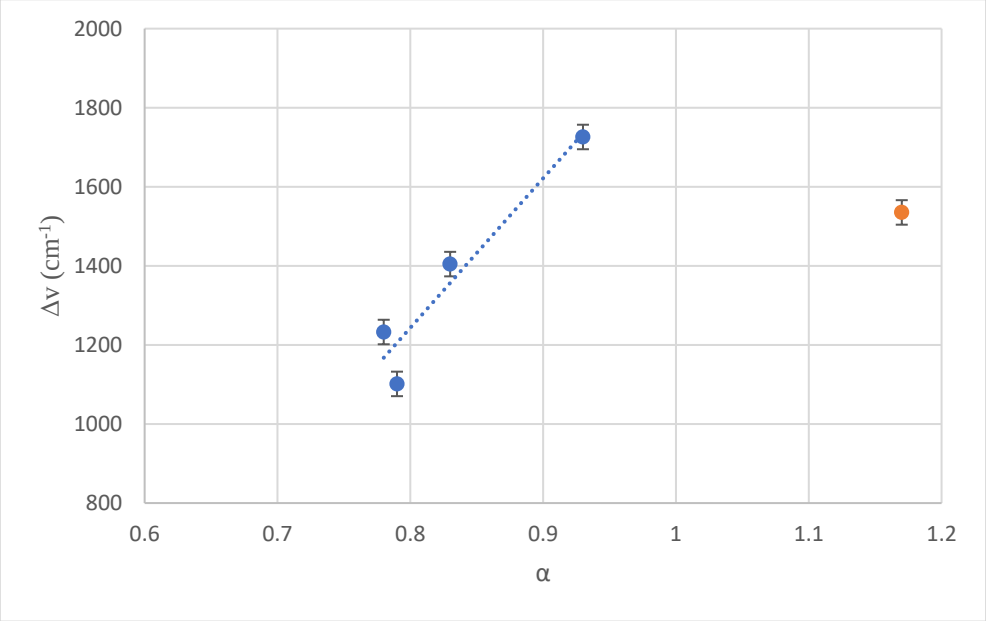

Figure 18: Δν against α for crystal violet, alcohol results in blue, Milli-Q water result in orange.

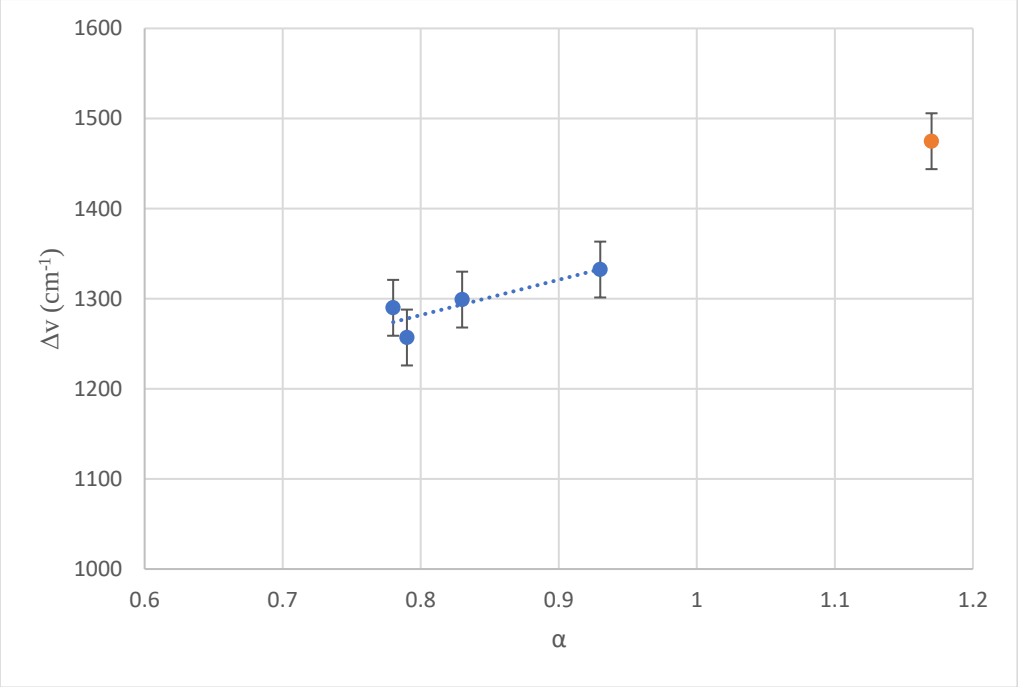

Figure 19: Δv against α for ethyl violet, alcohol results in blue, Milli-Q water result in orange.

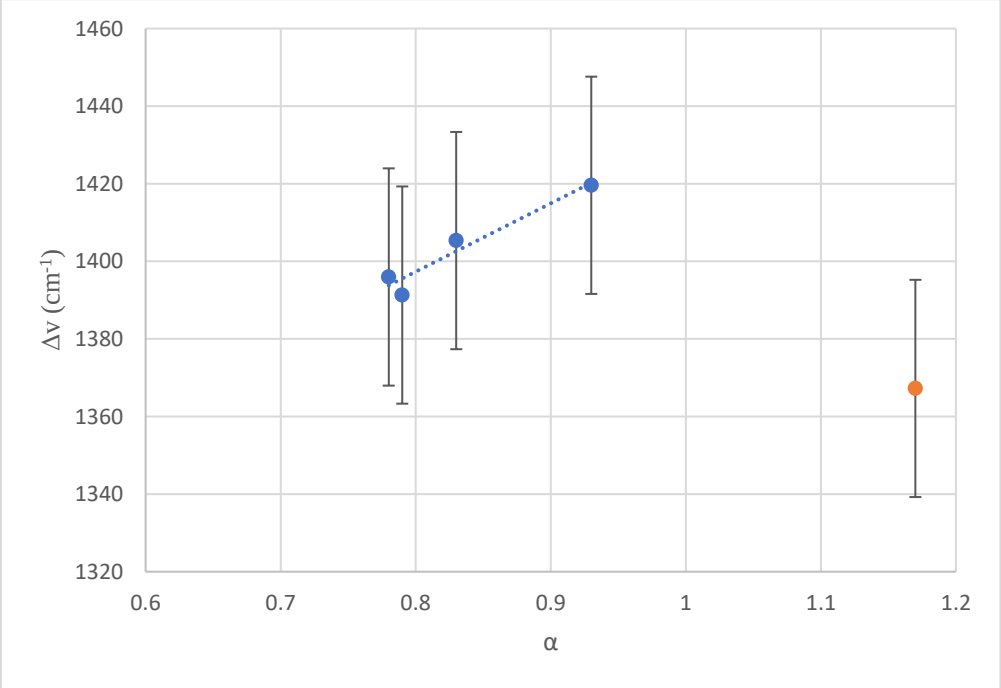

Figure 20: Δv against α for malachite green, alcohol results in blue, Milli-Q water result in orange.

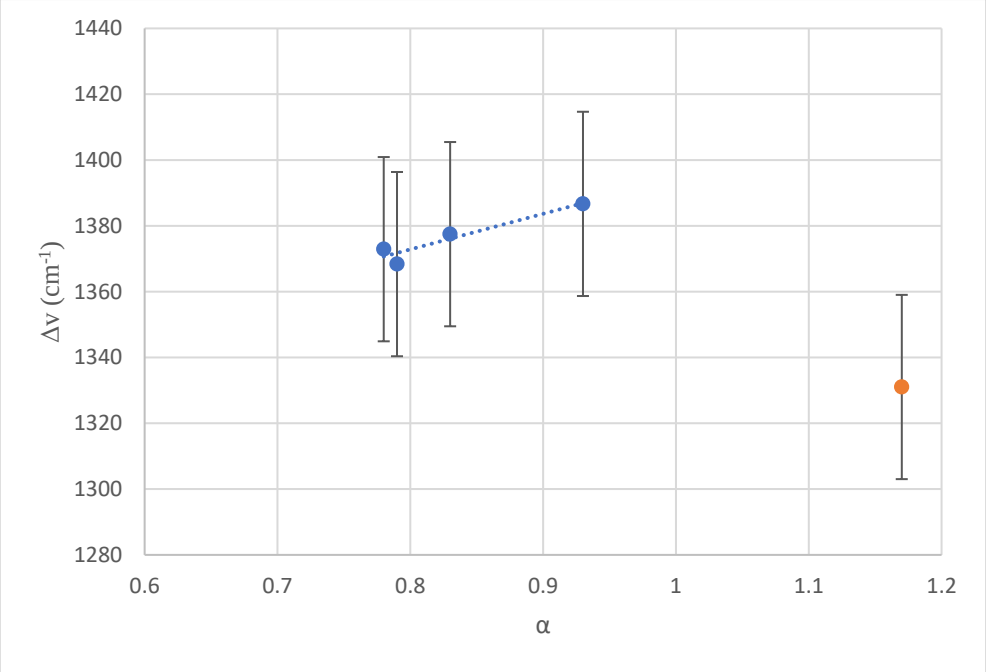

Figure 21: Δv against α for brilliant green, alcohol results in blue, Milli-Q water result in orange.

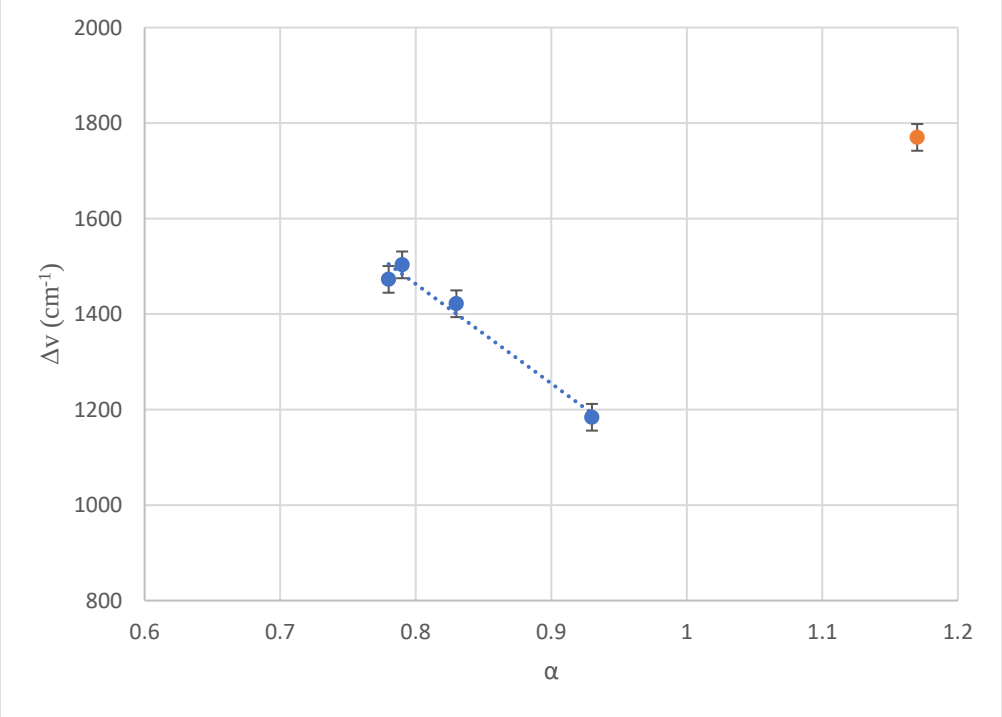

Figure 22: Δv against α for Victoria blue R, alcohol results in blue, Milli-Q water result in orange.

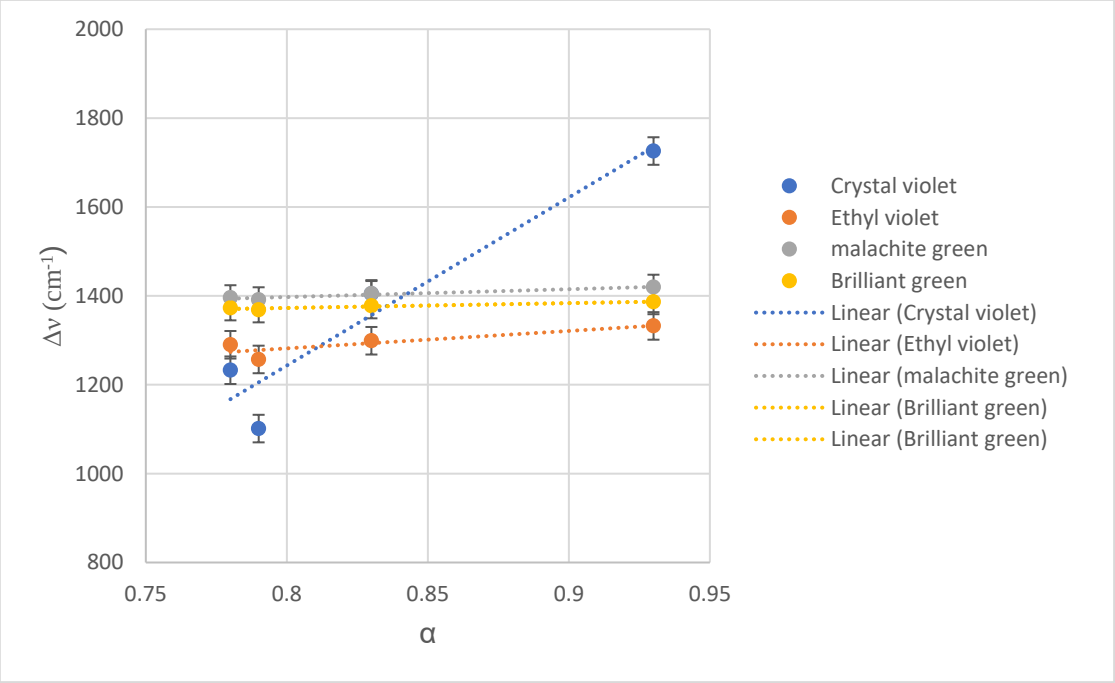

Figure 23: Overlapped graphs for the different dyes Δν against α, excluding Victoria blue R dye.

The parameter α, can be expressed as the ability of the solvent to form hydrogen bonds (3). For the dyes crystal violet, ethyl violet, malachite green and brilliant green, the trend in the results is positive and the highest separation value was found to correspond to the highest α value. With regards to Victoria blue R dye though a linear trend is present the degree of separation decreases with increasing α values.

These results are in line with those of Lewis, et al., (1) and Oliveira, et al., (3), though no explanation is given for the results of Victoria blue R. Note that in these graphs the outlier is from the solutions in butan-1-ol, suggesting that the value of α reported for this compound may be artificially high.

It can therefore be suggested that hydrogen bonds play a role in the breaking of the symmetry of the dyes crystal violet, ethyl violet, malachite green and brilliant green. To further analyse these dyes and how the relationship with the α parameter differs, the graphs have been overlaid (Figure 23). From Figure 23, more deductions can be made about the relationship and relating it to the dye structures.

Figure 23 shows that crystal violet has the steepest gradient of 3783 cm^{-1}, this decreases down the dyes, so ethyl violet has the next steepest gradient of 392.13 cm^{-1} then going to malachite green 176.17 cm^{-1} finally at brilliant green having the shallowest gradient of 108.25 cm^{-1}. Taking these values, and relating them to the dye structure, it can be seen that crystal violet has 3 auxochromes of $N(CH_3)_2$, so each of the nitrogen atoms is able to hydrogen

bond with the solvent. In ethyl violet, although there are 3 nitrogen atoms available for hydrogen bonds to occur with they are more sterically hindered, as there are two ethyl groups attached to the nitrogen, compared with methyl groups in crystal violet.

This trend continues with malachite green and brilliant green. Whereas crystal violet and ethyl violet had 3 auxochromes, malachite green and brilliant green only have 2 auxochromes reducing the opportunity to create hydrogen bonds. After this the reason deduced for brilliant green having the shallowest gradient is the same as ethyl violet, that the two ethyl groups attached the nitrogen atoms are hindering the availability of those nitrogens to take part in hydrogen bonding.

The π* parameter shows similar results for the dyes as the α parameter did. Figures 24-18 show Δν, as a function of π*.

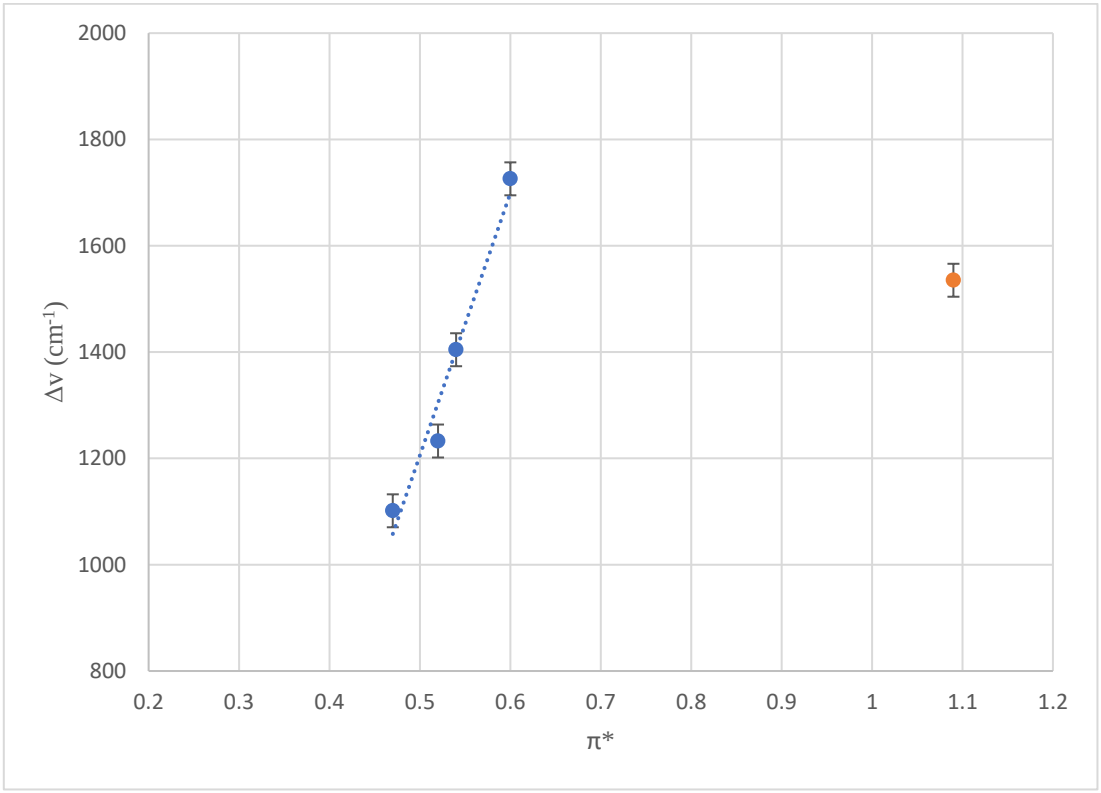

Figure 24: Δν against π* for crystal violet, alcohol results in blue and Milli-Q water result in orange.

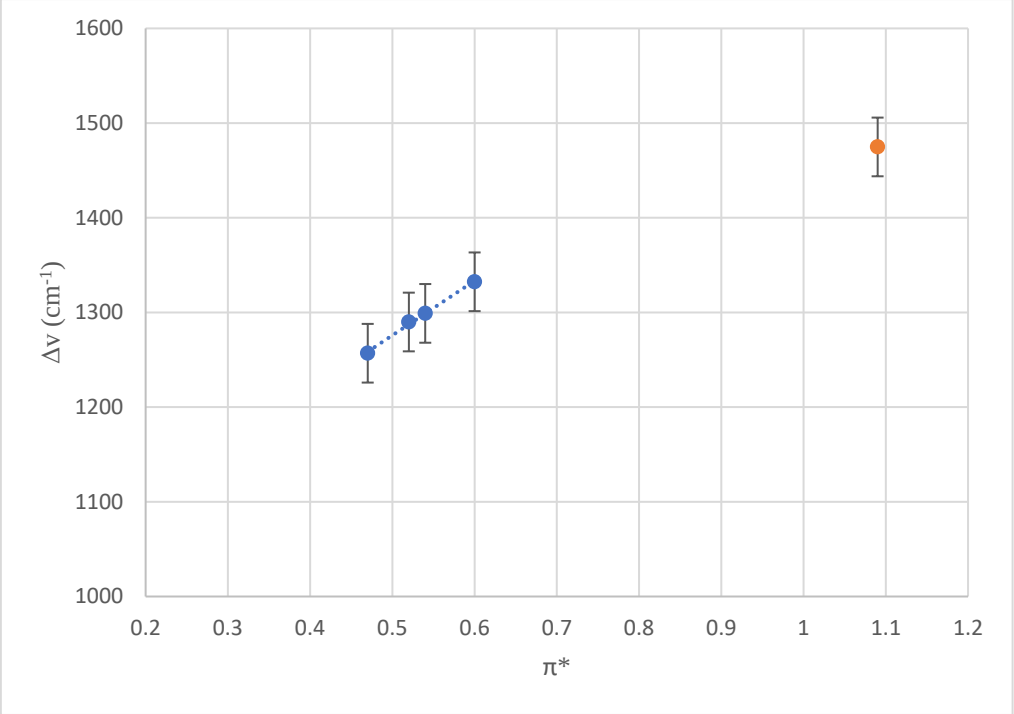

Figure 25: Δv against π* for ethyl violet, alcohol results in blue and Milli-Q water result in orange.

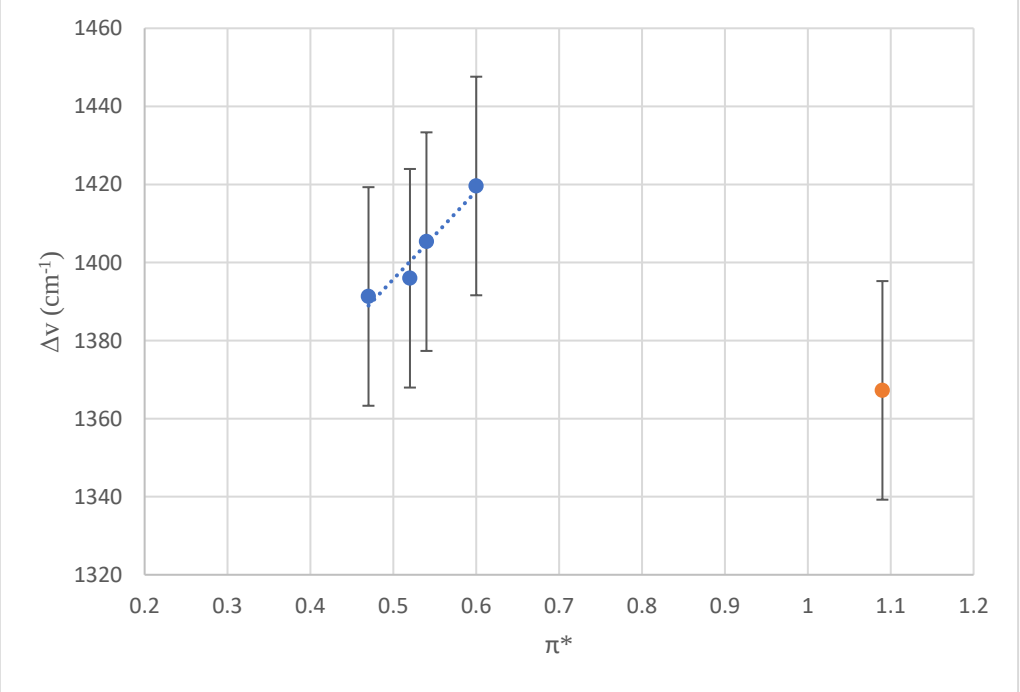

Figure 26: Δv against π* for malachite green, alcohol results in blue and Milli-Q water result in orange.

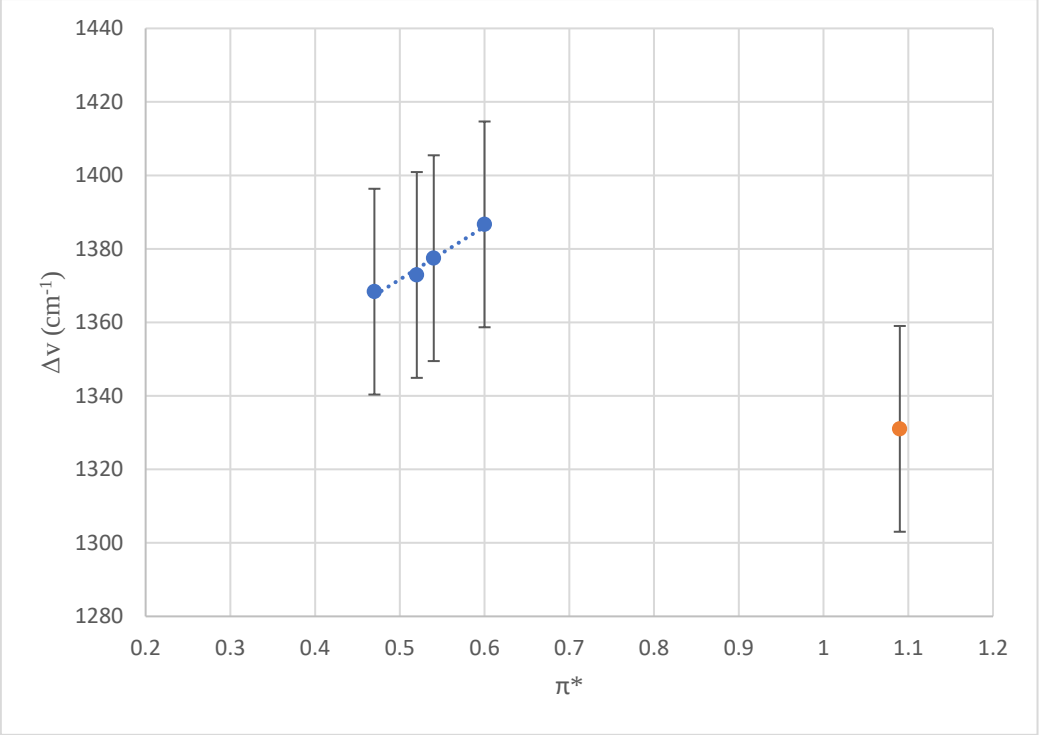

Figure 27: Δv against π* for brilliant green, alcohol results in blue and Milli-Q water result in orange.

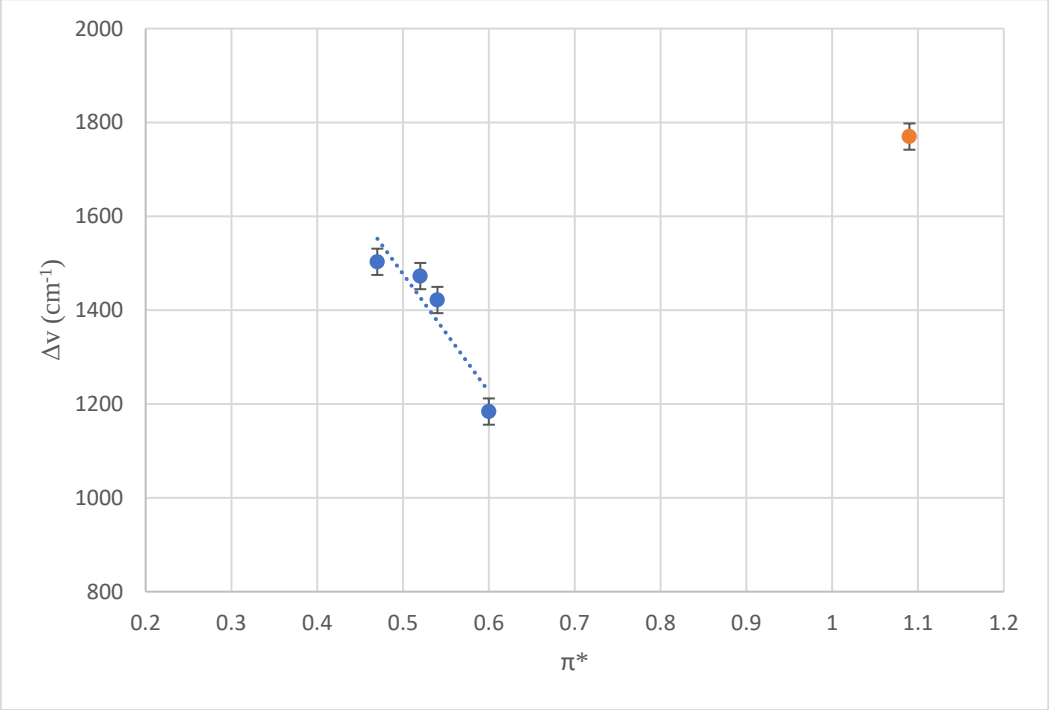

Figure 28: Δv against π* for Victoria blue R, alcohol results in blue and Milli-Q water result in orange.

π* is based on the solvents ability to induce dipoles in the solute (53). In the case of these dyes especially with crystal violet and ethyl violet the interaction is dipole-induced dipole. Crystal violet and ethyl violet fall into a category known as octupolar molecules. This is where the molecule has multiple dipoles and hence it cannot be stated exactly where the dipole will occur (39).

For dyes crystal violet, ethyl violet, malachite green and brilliant green, reduction in symmetry seems to be caused by either hydrogen bonding or dipole-induced dipole interactions with the solvent. The breaking of the symmetry would result in the dye taking a form with a lower symmetry. The explanation as to why the second absorbance band is overlapped with the main absorption peak can be explained in terms of the solvation sheaths. Figure 29 shows the absorbance spectrum of crystal violet where the two absorbance bands are unresolved.

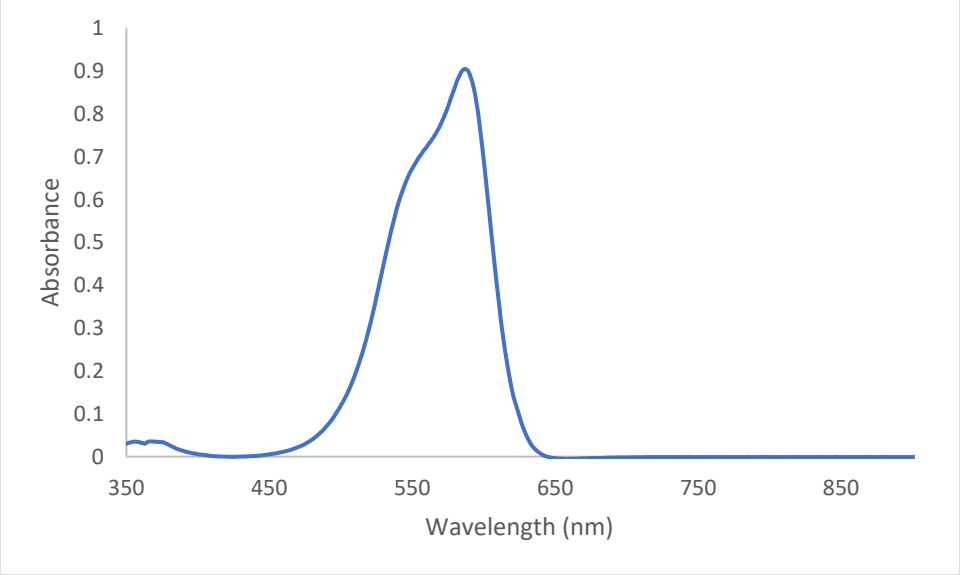

Figure 29: Absorbance spectrum of crystal violet in methanol.

When the symmetry is broken and the dye structure changes the solvation sheath changes around it. When the solute is excited, the solvent molecules must rearrange themselves around the solute and this causes a relaxation in the solvent cage. This results in the absorption bands blurring and overlapping, this compares to non-polar solvents where the bands will be resolved (46). There is clear blurring of the two absorption bands in Figure 29.

The final solvatochromic parameter to be considered is the hydrogen bond acceptor, β. Figures 30-34, show the relationship for each dyes degree of splitting against the parameter β.

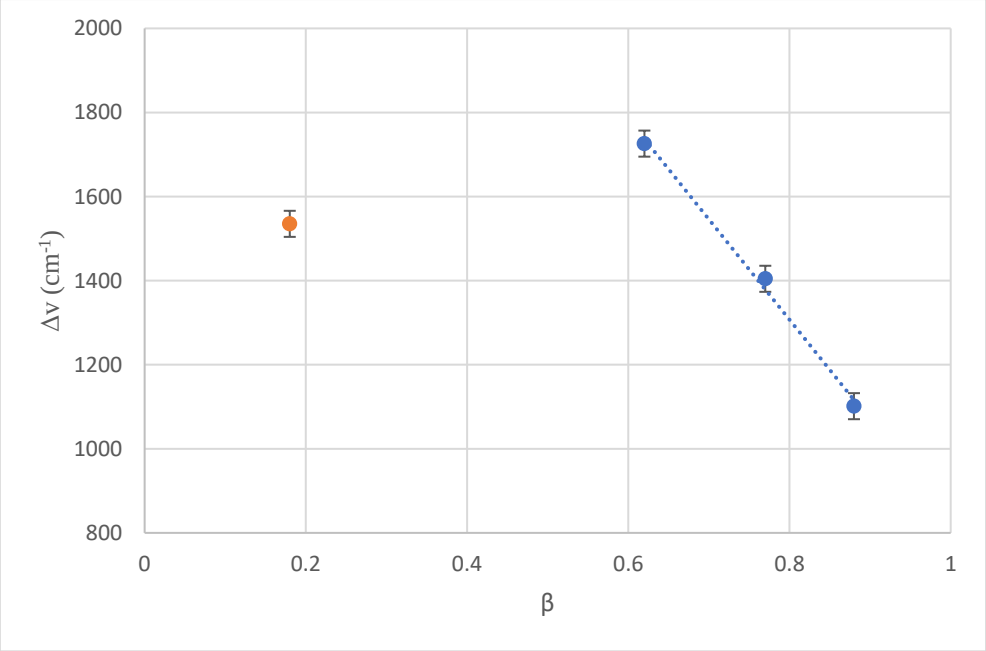

Figure 30: Δv against β for crystal violet, alcohol results in blue and Milli-Q water result in orange.

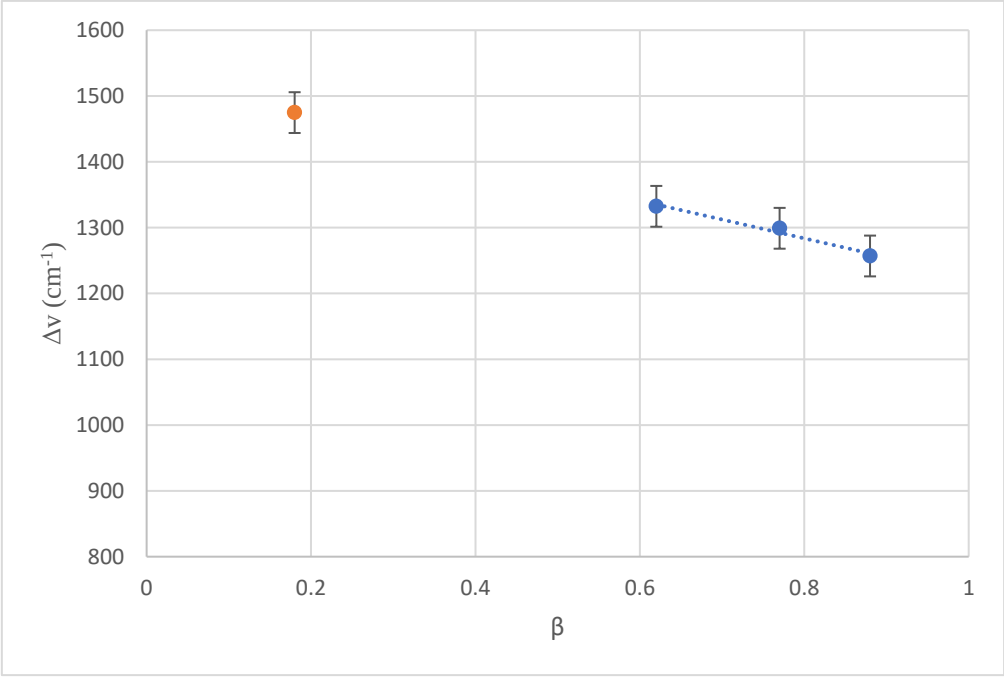

Figure 31: Δv against β for ethyl violet, alcohol results in blue and Milli-Q water result in orange.

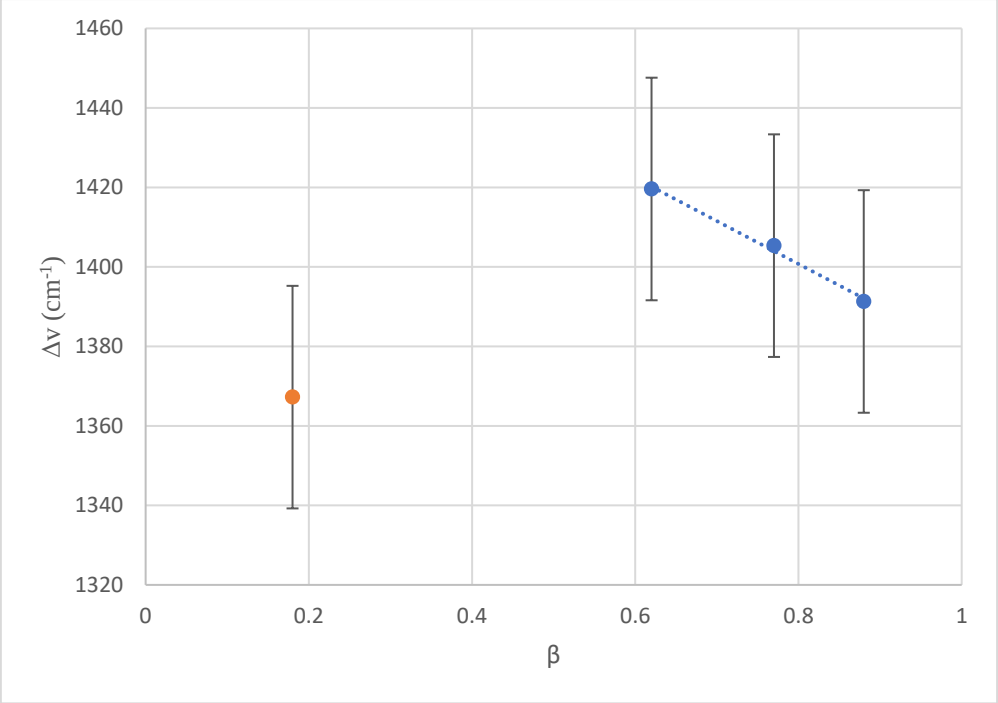

Figure 32: Δv against β for malachite green, alcohol results in blue and Milli-Q water result in orange.

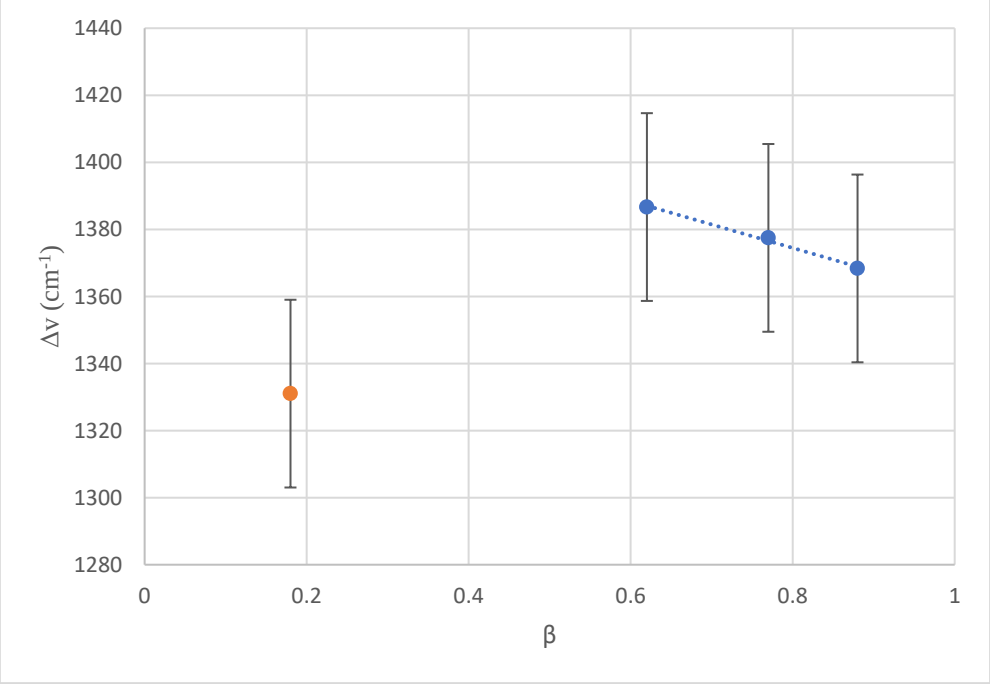

Figure 33: Δv against β for brilliant green, alcohol results in blue and Milli-Q water result in orange.

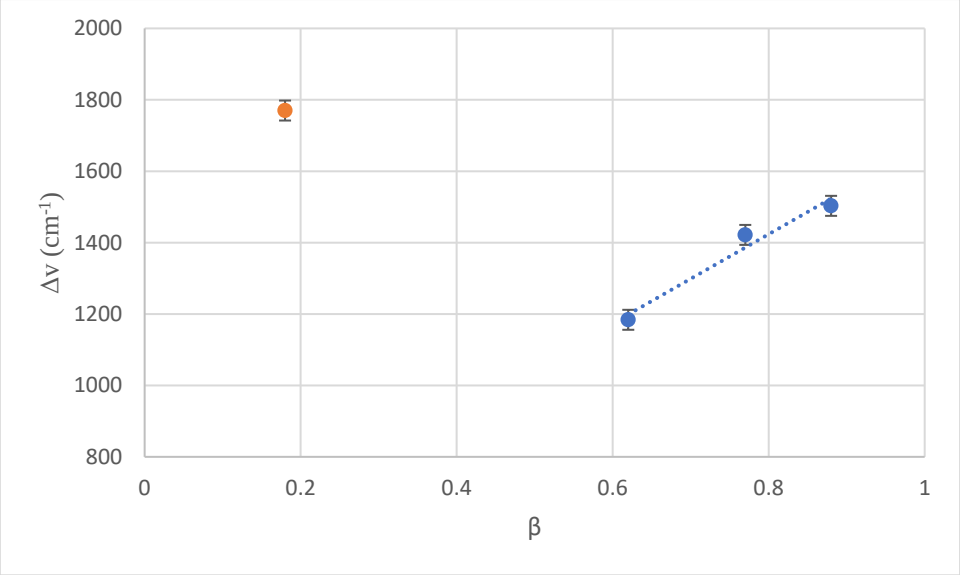

Figure 34: Δν against β for Victoria blue R, alcohol results in blue and Milli-Q water result in orange.

The linear relationship between β and $\Delta\nu$ is a surprising result, as the dyes crystal violet, ethyl violet, malachite green and brilliant green (Figures 30-33) do not have a suitable hydrogen to share in an interaction between the solute and solvent (3). The β parameter been how well the solvent accepts a proton from the solute to form a hydrogen bond.

Though currently the literature is unclear as to why the splitting of the bands for Victoria blue R, lies with the β parameter (Figure 34) over the other solvatochromic parameters. This compares to the other dyes where the splitting is due to the α, π* and dielectric constant. Though it is clear from the structure of Victoria blue R, that it has a hydrogen attached to a nitrogen that can part take in hydrogen bonding. As to why this has a dominating effect on the splitting of the two absorbance bands remains undetermined.

Therefore, for dyes crystal violet, ethyl violet, malachite green and brilliant green the highest splitting of the two bands within the alcohol class is found in methanol, and this decreases as the chain length increases. The opposite is found with Victoria blue R where the largest splitting of the two bands occurs in butan-1-ol.

So far, this section has reviewed the results for $\Delta\nu$, against the dielectric constant and the solvatochromic parameters at room temperature for the alcohol solvents. The Milli-Q water results identified in orange in the figures, tend to be anomalous and this is in line with what Lewis et al., found (1). The anomalous behaviour of the results in water, gives rise to the possibility that another phenomenon is taking place (3). This has been attributed to aggregation by Sheppard et al., (31). Conversely, Olivera et al., (3) found that the results in water are still concentration dependent. Therefore, aggregation would not be able to occur at the concentration used in this study.

This section has reviewed the relationship between the dye and the solvent and how this impacts an absorbance spectrum with regards to resolving the second absorbance band.

Temperature effects

Temperature can have an effect not only on the presence of the shoulder but also in any potential shifts in the λ_{max}. These shifts previously have been observed to be bathochromic shifts (54). Table 12 presents the λ_{max} values for the dyes in methanol at the 4 different temperature ranges selected. These temperatures are as follows:

- Temperature 1 – 40-50°C
- Temperature 2 – 30 -40°C
- Temperature 3 – 10-20°C
- Temperature 4 – 0-10 °C

These temperature ranges were achieved using a water bath or ice bath. Some challenges had to be overcome, since the heating and cooling of solutions had to be done in a fume cupboard to keep the alcohol vapours to a minimum. This meant that once a solution was taken out of the water or ice bath and transferred into the cuvette, the temperature would increase or decrease initially very quickly. The large surface area of the cuvette also contributed to how quickly the solution cooled or heated. On average the change in the temperature of the solution during an absorbance scan was 4°C. Therefore, not all temperature values correspond to exactly the temperature ranges.

Table 12: λ_{max} of dyes in methanol, at the 4 different temperature ranges.

	λ_{max} ±0.3 (nm) (average temperature, °C)			
	Temperature 1	Temperature 2	Temperature 3	Temperature 4
Crystal violet	586.0 (36.75)	587.0 (31.80)	587.0 (15.00)	588.0 (10.40)
Ethyl violet	588.0 (39.65)	589.0 (32.40)	588.0 (15.20)	588.0 (9.15)
Malachite green	617.0 (40.05)	619.0 (32.25)	619.0 (15.25)	619.0 (9.00)
Brilliant green	625.0 (37.45)	626.0 (31.35)	627.0 (15.01)	626.0 (7.95)
Victoria blue R	616.0 (38.45)	616.0 (32.40)	617.0 (14.95)	617.0 (6.65)

The trend seen in Table 12 is that with decreasing temperature there is a bathochromic shift of the λ_{max}. This trend is greatest for the dye crystal violet and less obvious with the others. This trend of bathochromic shifts in the λ_{max} with decreasing temperature can also be seen across the other alcohol solutions studied. These results are in agreement with the literature and are

explained as that as the temperature is decreased the second excited state becomes increasingly stabilized (54).

This stabilization cannot be seen for the dyes in water. The results in Table 13 present the opposite trend where a hypsochromic shift of the λ_{max} for the crystal violet, ethyl violet, malachite green and brilliant green is observed.

Table 13: λ_{max} of the dyes in Milli-Q at the 4 different temperatures.

	$\lambda_{max} \pm 0.3$ (nm) (temperature, °C)			
	Temperature 1	Temperature 2	Temperature 3	Temperature 4
Crystal violet	591.0 (44.30)	592.0 (35.70)	589.0 (10.00)	598.0 (7.40)
Ethyl violet	595.0 (43.00)	595.0 (35.00)	594.0 (11.9)	594.0 (6.35)
Malachite green	617.0 (41.60)	617.0 (35.00)	617.0 (12.80)	617.0 (7.90)
Brilliant green	626.0 (40.70)	626.0 (35.10)	625.0 (13.05)	625.0 (6.75)
Victoria blue R	613.0 (44.70)	612.0 (35.50)	625.0 (12.17)	625.0 (6.15)

This hypsochromic shift may be due the structure of water becoming more ordered as the solvent approaches its freezing point of 0°C. Water is able to form cage like structures not only in the solid phase but also in the liquid phase (55). It is interesting to note that Victoria blue R shows the same trend of bathochromic shift which is expected within the alcohol solvents with decreasing temperature. As to why this is the case currently no explanation can be given.

For the majority of the dyes in water, not only is there a bathochromic shift in the λ_{max} the shoulder becomes less pronounced as temperature decreases. Figure 35 presents the dye crystal violet at the higher temperatures and Figure 36 at lower temperatures.

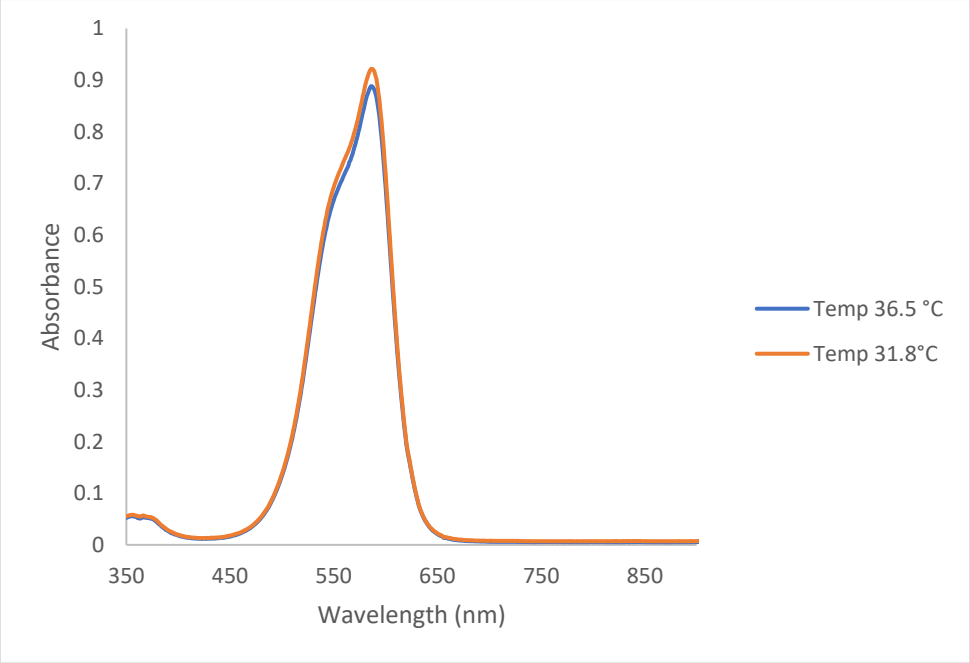

Figure 35: Absorbance spectra of crystal violet in methanol at higher temperatures.

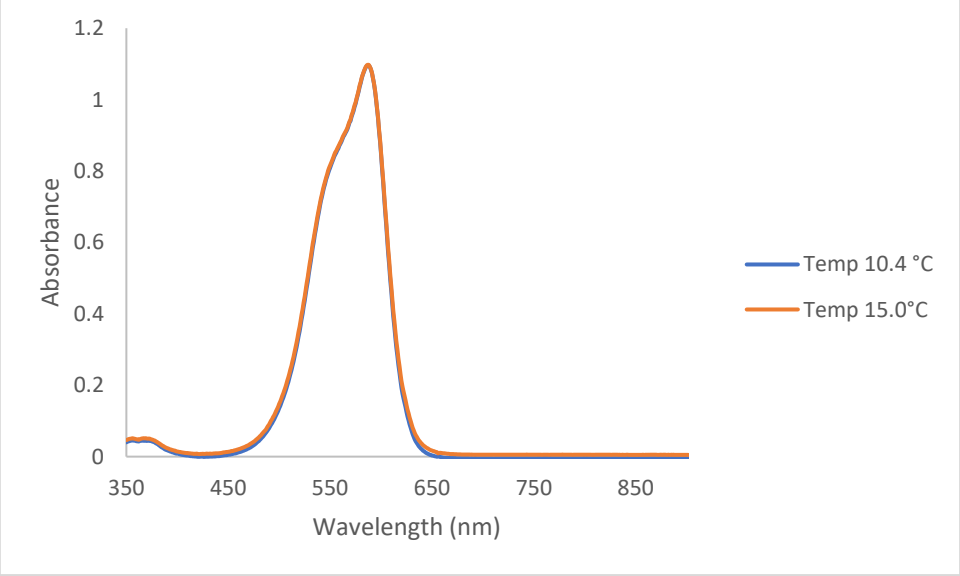

Figure 36: Absorbance spectra of crystal violet in methanol at low temperatures.

Figures 35 and 36, provide the absorption spectra of crystal violet at the different temperatures. However, it is difficult to see the shift in λ_{max} due to the intensities of the bands being similar to each other and the shifts being small in comparison to the width of the bands. Discussion of temperature effects on intensities is provided in the extinction coefficient section. Even with increasing

temperature, the intensity of the shoulder seems to remain constant or have a constant relationship with the intensity of the λ_{max}. Therefore, these bands cannot be related to partially resolved Frank-Condon progressions within single electronic states (1).

It is not obvious from the spectra alone that the shoulder diminishes with decreasing temperature. To provide evidence that the shoulder is merging into the main absorption peak, the degree of splitting $\Delta\nu$, has been plotted against the temperature for the dye crystal violet in methanol as an example (Figure 37).

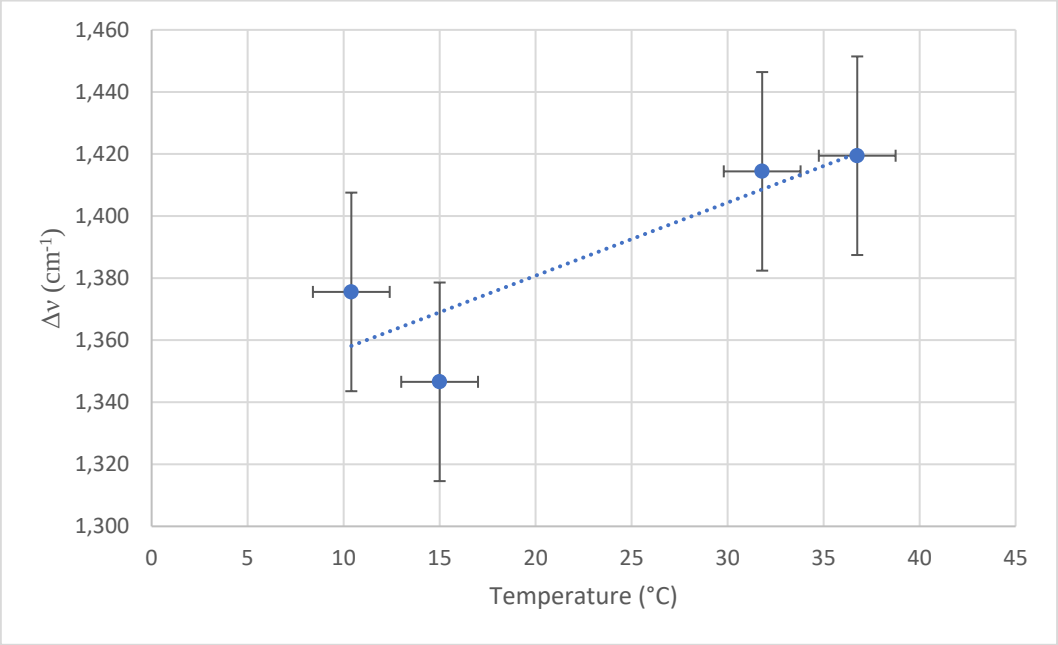

Figure 37: Δν against temperature for crystal violet in methanol.

This figure shows that the shoulder becomes more resolved as temperature increases. The error bars in the x axis direction relate to the temperature change that occurs during the absorbance scan. Following on from this the degree of splitting has been plotted against the solvatochromic parameters as in the previous section on solvent effects.

Previously it was seen that the degree of splitting increased as α increased. It can be presumed then that this trend will continue for the high temperatures. Figures 38-42 present this data.

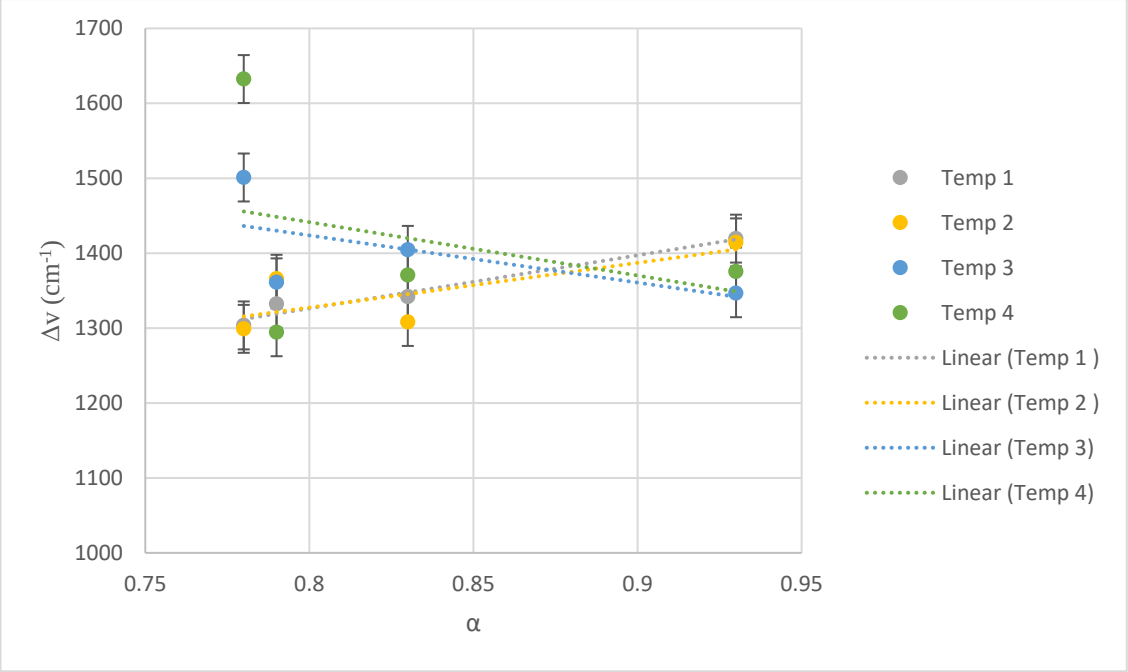

Figure 38: Δv against α for crystal violet, alcohol results produced at the different temperature ranges.

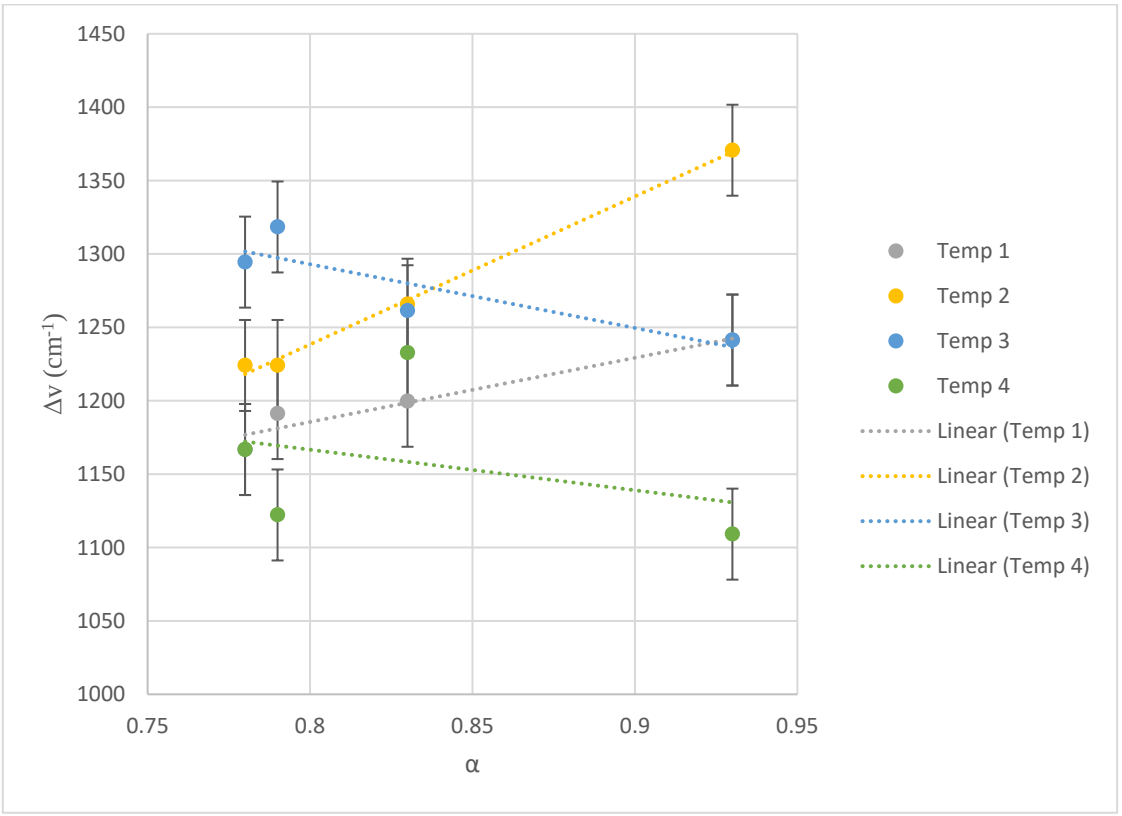

Figure 39: Δv against α for ethyl violet, alcohol results produced at the different temperature ranges.

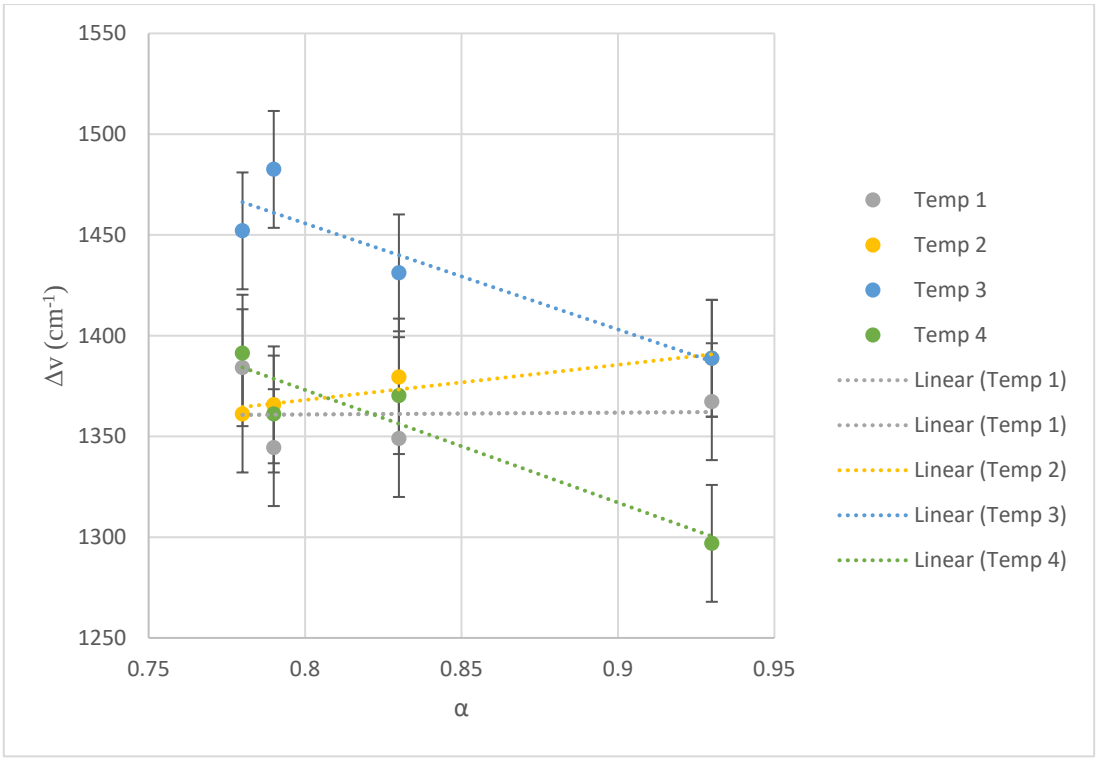

Figure 40: Δv against α for malachite green, alcohol results produced at the different temperature ranges.

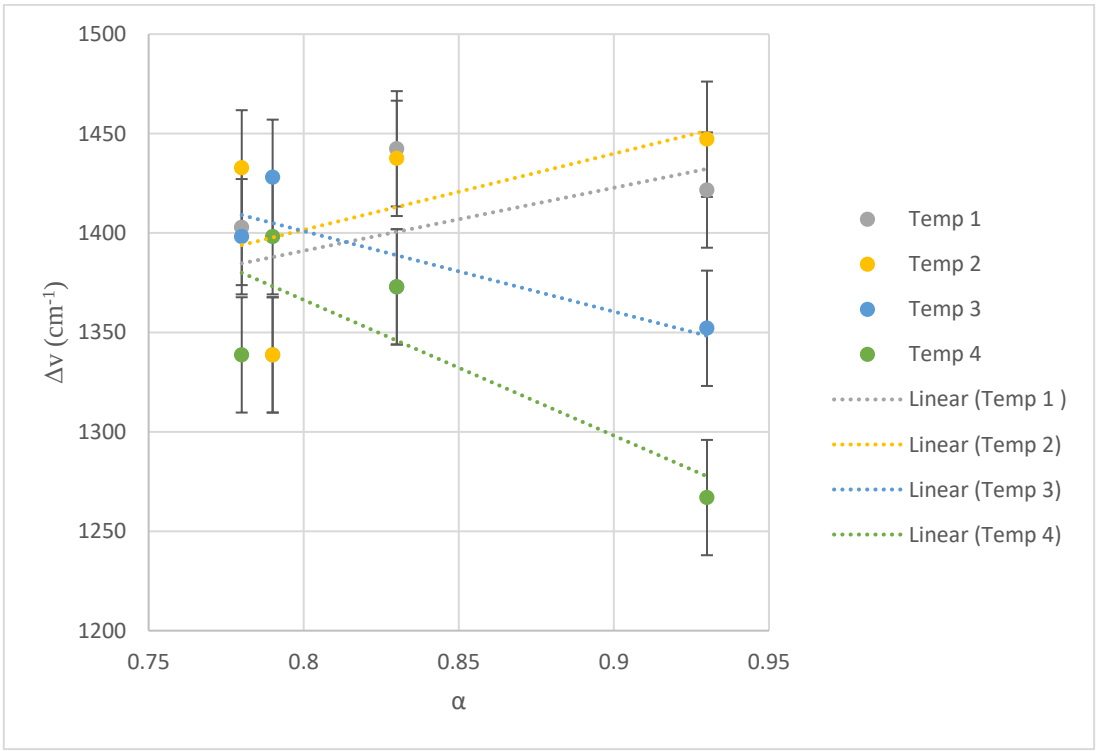

Figure 41: Δv against α for brilliant green, alcohol results produced at the different temperature ranges.

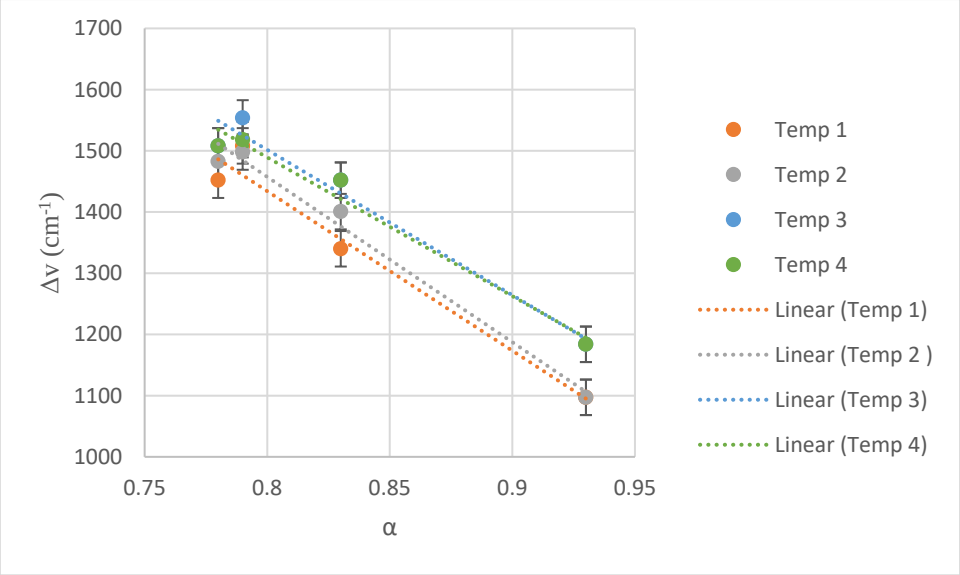

Figure 42: Δν against α for Victoria blue R, alcohol results produced at the different temperature ranges.

The most interesting aspect from Figures 38-42, is that at low temperatures there is a complete change in the direction of the gradient. With the high temperature work the degree of splitting increases with increasing α values, at the low temperature the degree of splitting decreases with increasing α values. Victoria blue R, presents again interesting data that even with the changes in temperature the trend is very much remains that as the α value increases the degree of splitting decreases.

The error bars seen on Figures 38-42 as previously mentioned in the solvent effects section, were calculated by taking the uncertainty value found in the precision section and using the extreme values of uncertainty and converting through to wavenumbers then finding the difference between the λ_{max} value in wavenumbers and the two values take to be the limits of the uncertainty. The size of these error bars is such that the change in the gradient of these graphs cannot be attributed to experimental error alone.

It would be reasonable to presume that these trends would follow for the π* parameter. It has previously been found in this study that the dyes crystal violet, ethyl violet, malachite green and brilliant green all had positive linear relationship with the π* parameter. Figures 43-47, present how the relationships between Δν and π* changes with temperature for the dyes.

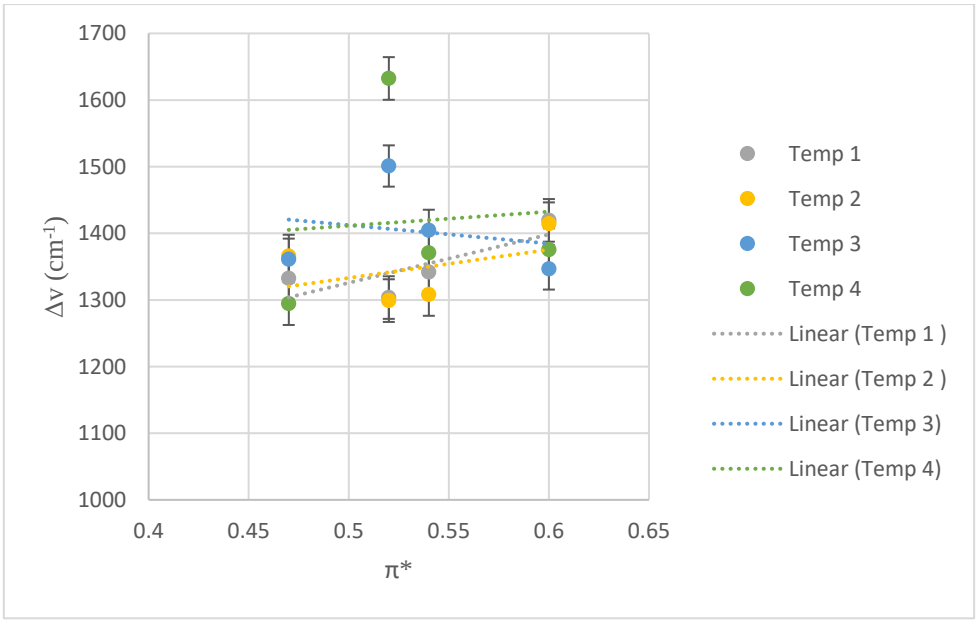

Figure 43: Δv against π* for crystal violet, alcohol results produced at the different temperature ranges.

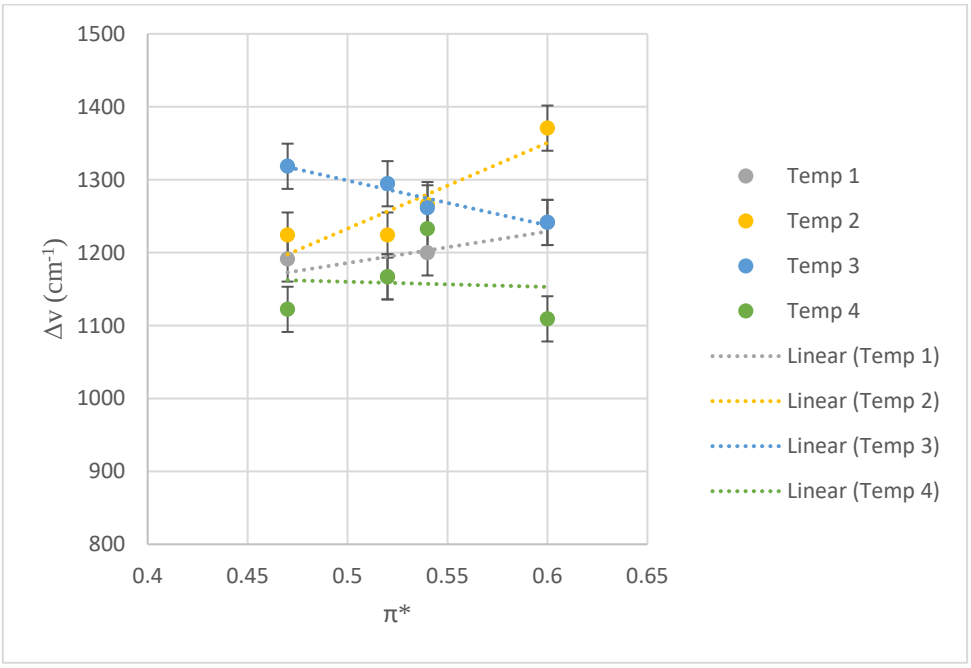

Figure 44: Δv against π* for ethyl violet, alcohol results produced at the different temperature ranges.

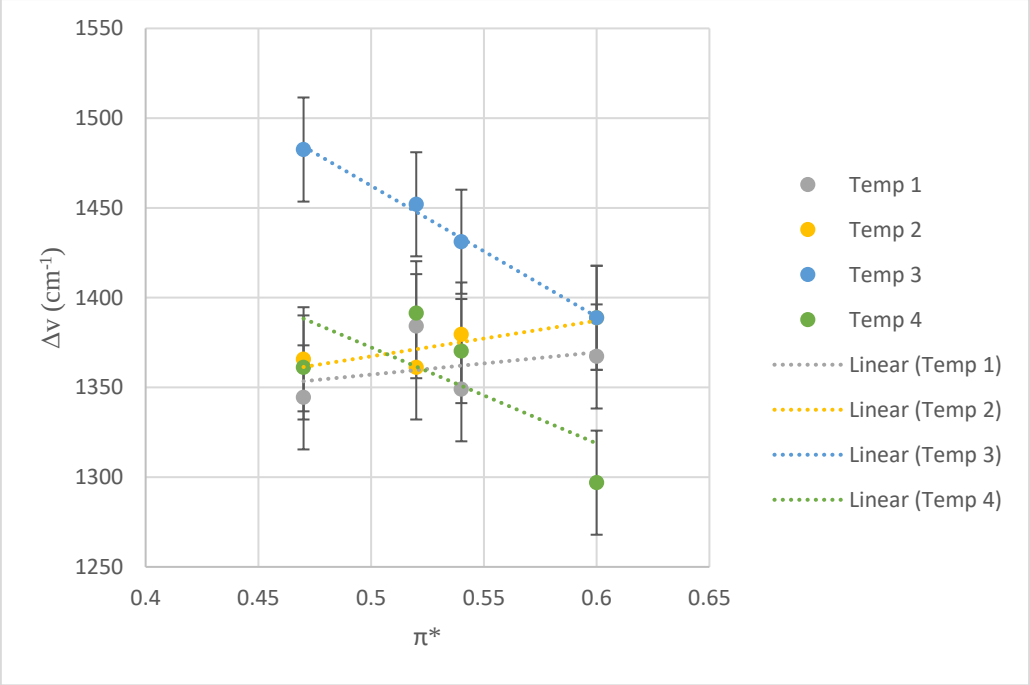

Figure 45: Δv against π* for malachite green, alcohol results produced at the different temperature ranges.

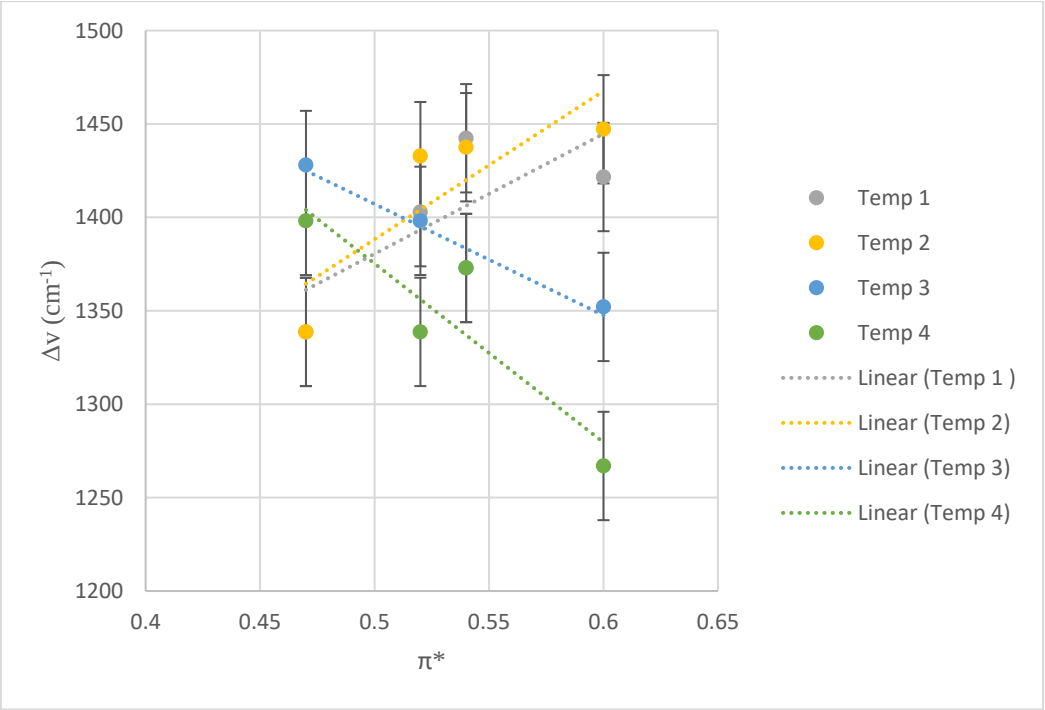

Figure 46: Δv against π* for brilliant green alcohol results produced at the different temperature ranges.

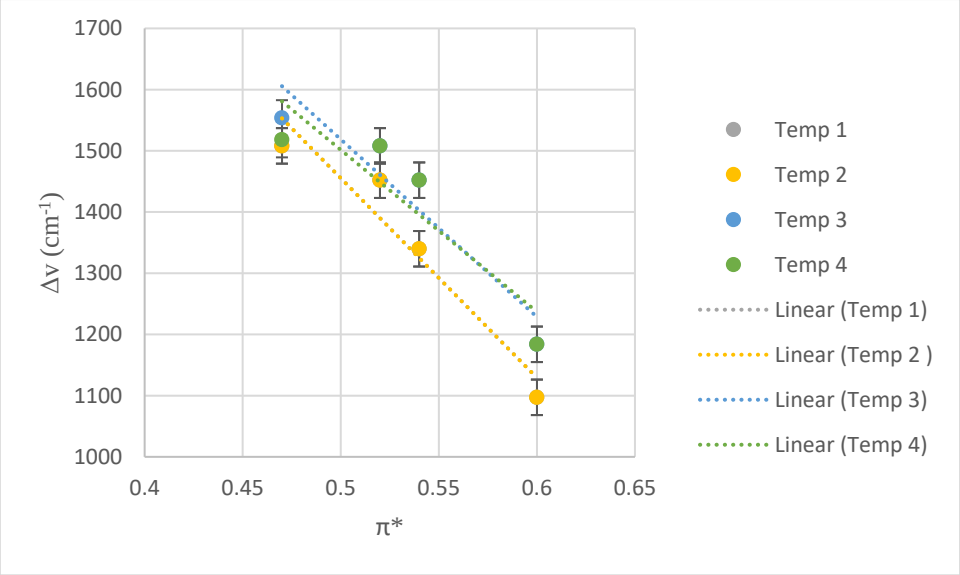

Figure 47: Δv against π* for Victoria blue R, alcohol results produced at the different temperature ranges.

Figures 43-47, show that the presumption made holds true, that the same trends are seen as for the α parameter.

Moving on to look at the dielectric constant graphs Figures 48-52.

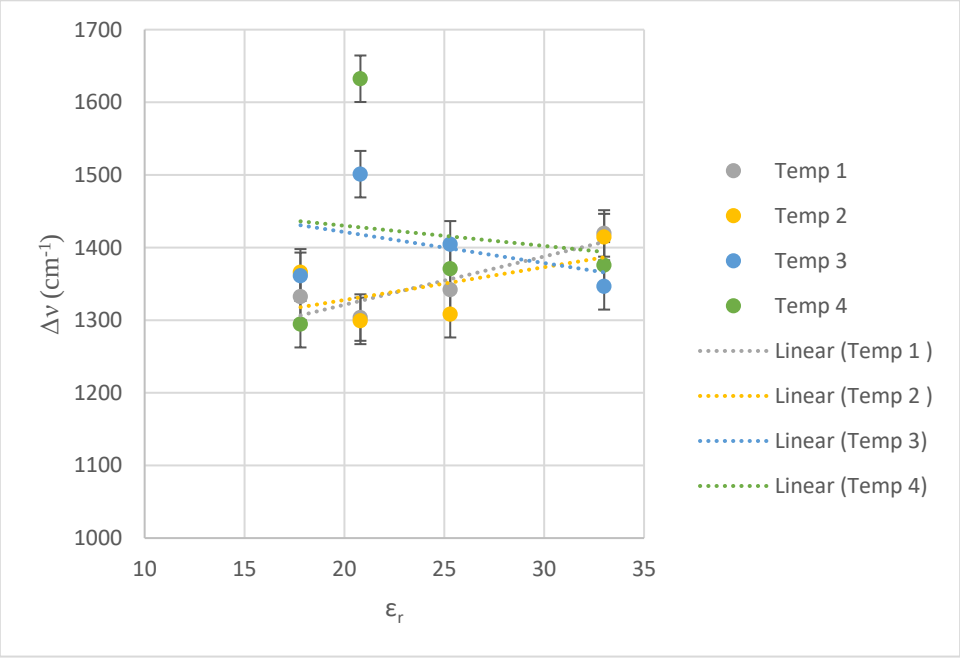

Figure 48: Δv against ε_r for crystal violet, alcohol results produced at the different temperature ranges.

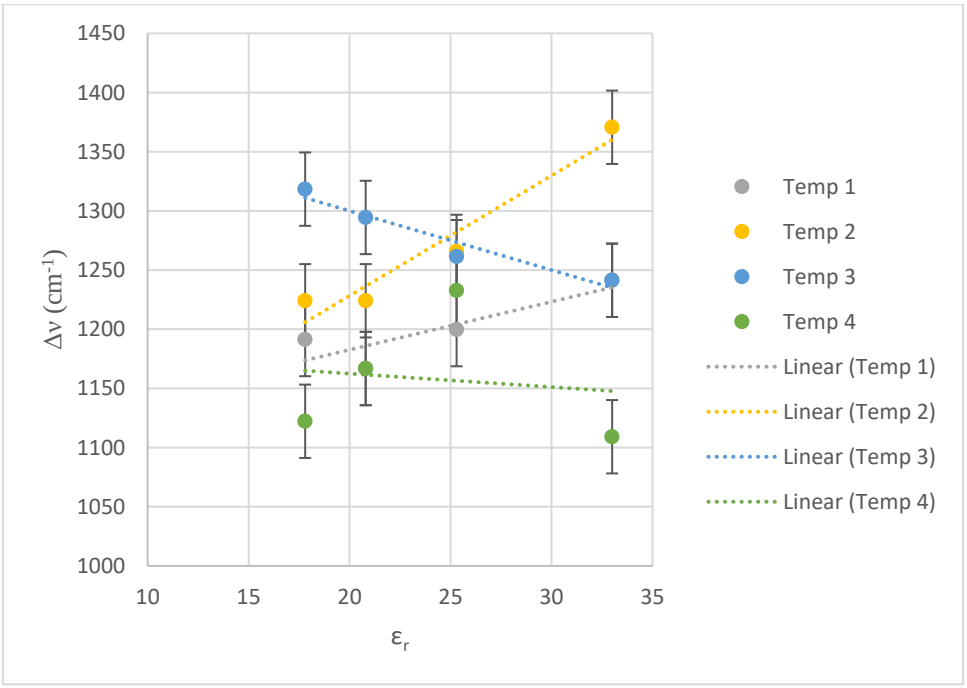

Figure 49: Δv against ε_r for ethyl violet, alcohol results produced at the different temperature ranges.

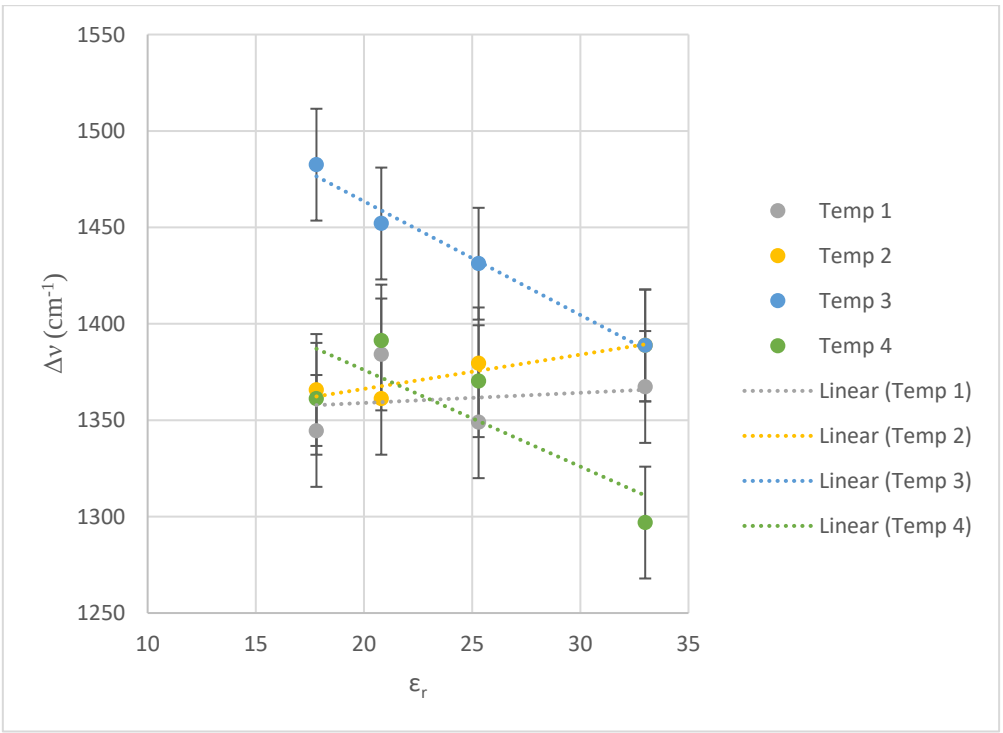

Figure 50: Δv against ε_r for malachite green, alcohol results produced at the different temperature ranges.

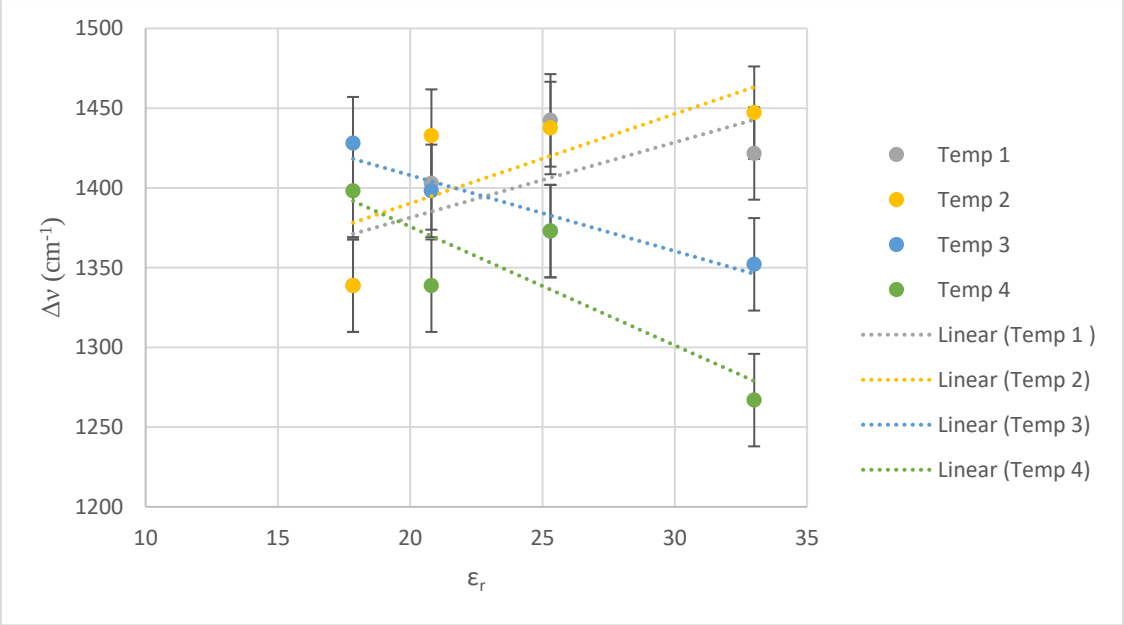

Figure 51: Δν against ε_r for brilliant green, alcohol results produced at the different temperature ranges.

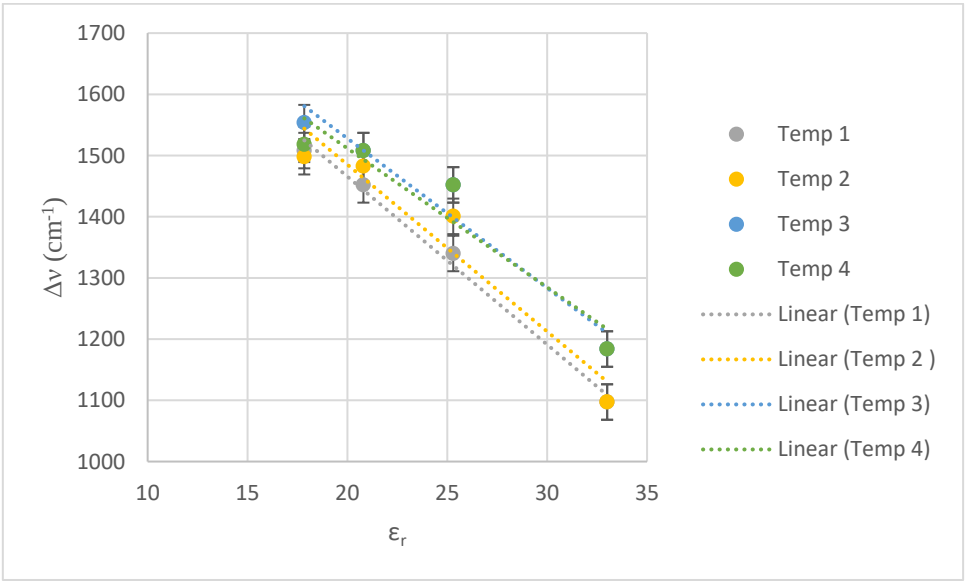

Figure 52: Δν against ε_r for Victoria blue R, alcohol results produced at the different temperature ranges.

Again, the previous relationship that was seen for the dyes with the α and π* parameter holds, with the dielectric constant. Finally, the degree of splitting at the different temperatures was plotted against the β parameter values (Figures 53-57).

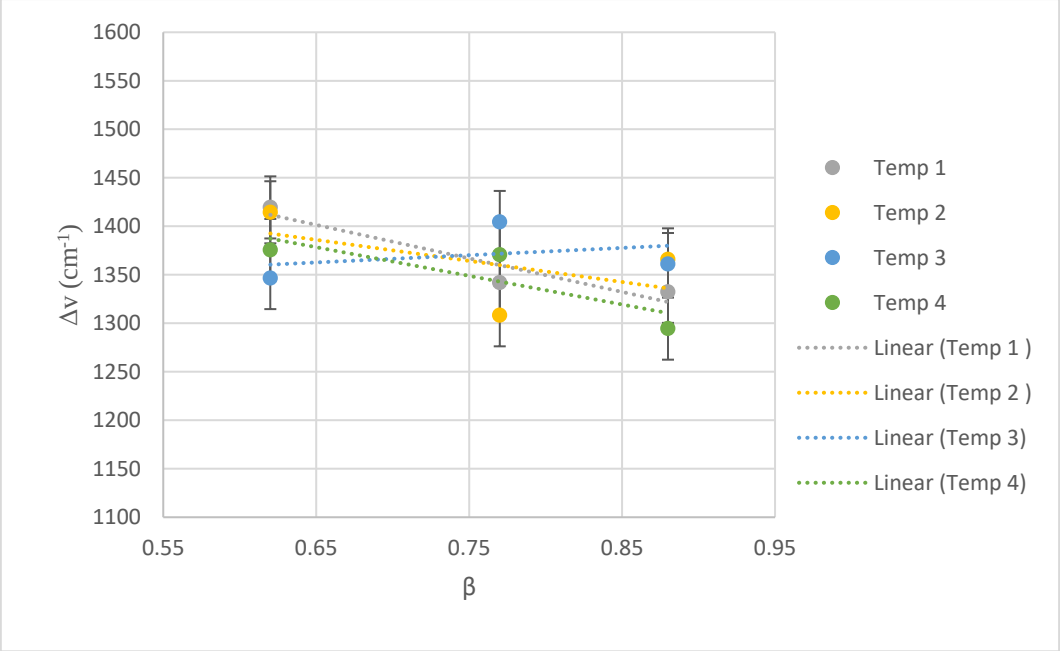

Figure 53: Δv against β for crystal violet, alcohol results produced at the different temperature ranges.

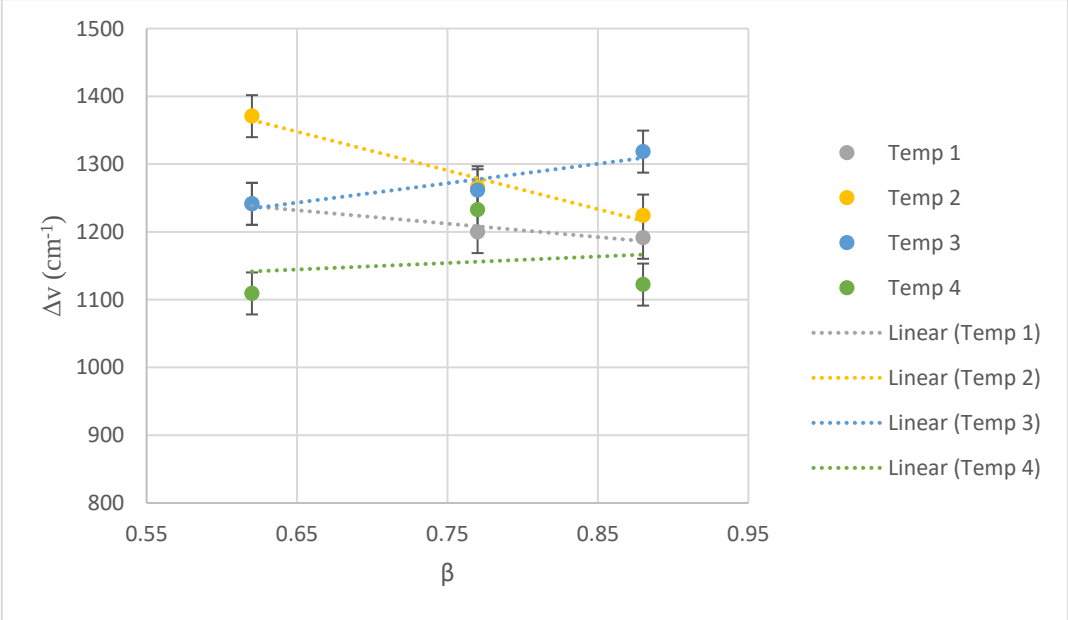

Figure 54: Δv against β for ethyl violet, alcohol results produced at the different temperature ranges.

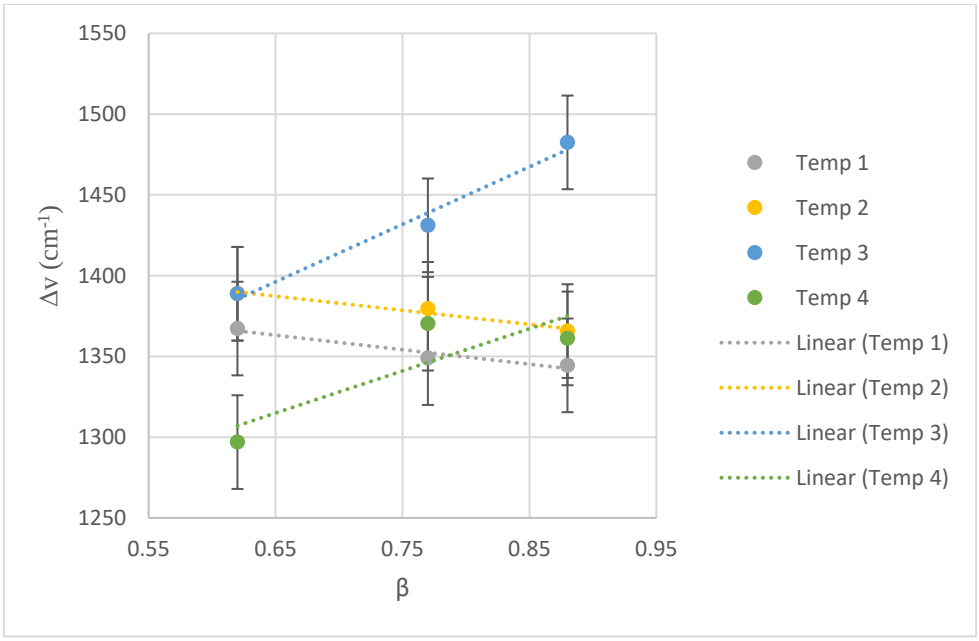

Figure 55: Δv against β for malachite green, alcohol results produced at the different temperature ranges.

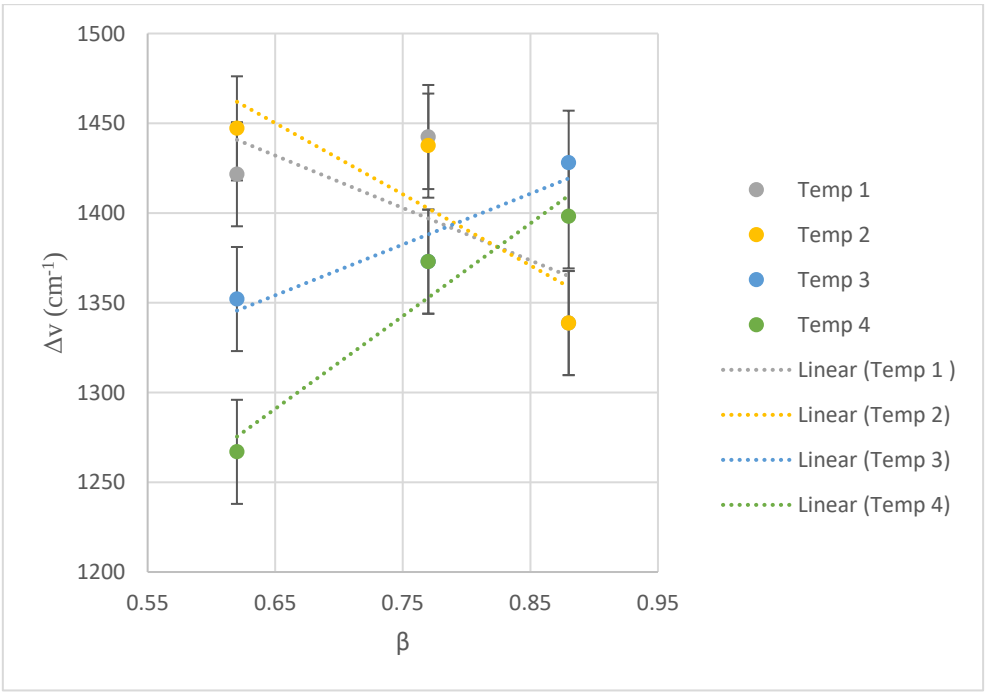

Figure 56: Δv against β for brilliant green, alcohol results produced at the different temperature ranges.

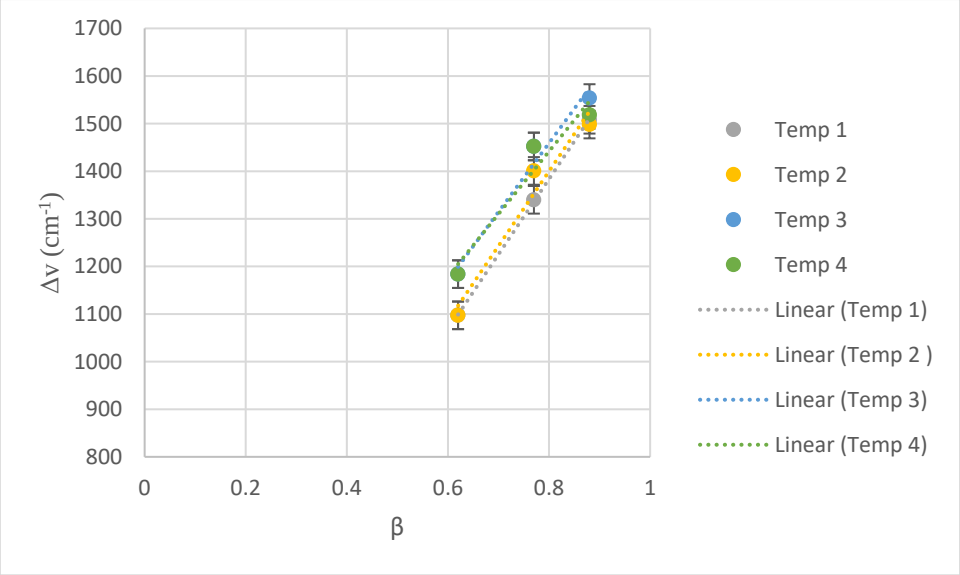

Figure 57: Δv against β for Victoria blue R, alcohol results produced at the different temperature ranges.

As mentioned in the solvent effects section the parameters α and β are opposite of each other. Experimental data from this work bears this out as Figures 53-57 show the opposite the trends to those in Figures 38-42.

A note of caution is advised with the solvatochromic graphs as currently there the effect of temperature upon the parameter α, β and π* is unknown. However, whilst peak splitting as a function of solvatochromic parameter has been previously reported (1), this is the first experimental data showing the effect of temperature upon these systems. Two inferences can be extracted from what the solvatochromic graph show in terms of the relationship between temperature, dye and solvent. Firstly, it is possible that α, β and π* graphs show that there is a link between the solvent and temperature. It is therefore likely that this link, is caused by low temperatures where other phenomena become the predominate interaction between the solvent-solvent rather than the solvent-dye. It may just be as possible that these graphs suggest that there is a link between the dye and temperature. How temperature links directly to low temperature would require further investigation.

It is important now to consider in more detail how temperature effects the absorbance spectrum. It is a key that for the alcohol series temperature will influence the alcohols ability to solvate, this links to the solvatochromic graphs suggesting that there is a link between solvent and temperature. It is known for methanol that at low temperatures it will self-associate, therefore, the number of methanol monomers capable of solvating the dye would decrease. This has the impact of decreasing the interactions between the solvent and dye, the decrease in the interaction would result in only 1 form present with 1 symmetry point group (1). That symmetry would be indicated to be the D_3 propeller shape as detailed within the symmetry section, this is backed other studies

undertaken (1, 34). In general, it seems that $\Delta\nu$ decreases as temperature is lowered, and this study has proven that to be the case. Hence, for other alcohols in the series it can be conceivably be hypothesised that the mechanism of decreasing monomers as temperature is lowered for methanol can be envisaged with the other alcohols studied. This is supported with the experimental data shown in this chapter.

Obtaining 1 peak present on the absorption spectrum of crystal violet in methanol has been achieved by Korppi-Tommola et al., (17) was achieved by using a thermostatic cell holder and having liquid nitrogen flow around the cell. As this study did not have a thermostatic cell holder due to the expense to use, was not attempted to be replicated and therefore cannot say for certain that this is reproducible. From the results that have been obtained it can be suggested that the shoulder would diminish at a certain temperature. This is limited by the finding that only crystal violet has been investigated at such low temperatures and to be able to conclude that this occurred for all the triarylmethane dyes would need further investigation.

Extinction coefficients

Though this section will discuss the extinction coefficients of the dyes, with focus at how the solvent and temperature effect these values. The relationship between extinction coefficient and absorbance is given by the rearranged equation below:

$$\varepsilon = \frac{A}{c \cdot l}$$

Where A is the absorption coefficient, c is the concentration and l is the path length of the cell. Table 14, shows the λ_{max} of each dye in the solvent at room temperature and the calculated extinction coefficients. Figure 58, shows the extinction coefficients against temperature for the dye crystal violet in methanol.

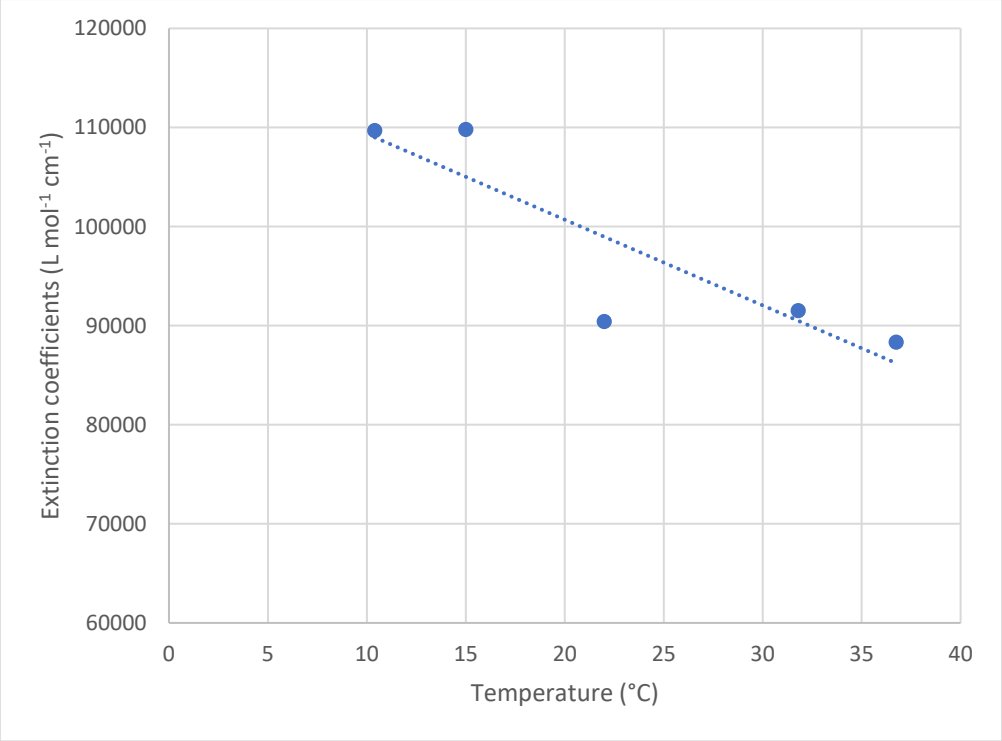

Figure 58: Extinction coefficients against temperature for crystal violet in methanol.

All the extinction coefficients in Table 14 and Figure 58 have an uncertainty of ± 0.187 L mol^{-1} cm^{-1}. The wavelengths in Table 14, have an uncertainty of ± 0.32 nm. The uncertainty in the extinction coefficients cannot be expressed in Figure 58, as the markers for the points are larger than the error bars. The uncertainties values were calculated by putting the uncertainties in the measurements (see section on precision) into the equation.

Although not a direct relationship it can be observed that as temperature decreases, the extinction coefficient increases as shown in Figure 58. This trend is also observed for the other dyes in the solvents conducted in this study.

The cause of this hyperchromic shift with decreasing temperature is unclear, but it may be related to the how the solvent is interacting with the dye molecule, as in the previous solvent effects section and temperature effects section. If the temperature can change the solvation properties so that only 1 symmetry form of the dye is present the form that gives rise to the lower wavelength, usually main peak, this would have the potential of increasing the extinction coefficients.

Previous work has suggested that at low temperatures, methanol will self-associate (1). This alters the solvent cage and how previously discussed the interaction of the solvent with the dye. Since the solvent at low temperatures interactions decrease only 1 symmetry form of the dye is present and this increases the absorbance value for that symmetry of the dye. At higher

temperatures the decrease in the extinction coefficients value has the potential of 2 causes. This relates to the chemical drift in the uncertainty section.

Table 14: λ_{max} and extinction coefficient for the dyes in all solvents at room temperature.

Solvent		Crystal violet	Ethyl violet	Malachite green	Brilliant green	Victoria blue R
Milli-Q	λ_{max} (nm)	590	595	617	625	613
	Extinction coefficient (L mol^{-1} cm^{-1})	69,510	39,583	109,470	36,546	21,660
Methanol	λ_{max} (nm)	587	590	619	626	617
	Extinction coefficient (L mol^{-1} cm^{-1})	90,400	105,810	164,740	104,590	56,394
Ethanol	λ_{max} (nm)	589	590	622	628	625
	Extinction coefficient (L mol^{-1} cm^{-1})	100,650	95,134	49,265	56,931	49,915
Propan-1-ol	λ_{max} (nm)	590	592	624	629	627
	Extinction coefficient (L mol^{-1} cm^{-1})	95,081	78,229	30,360	53,171	58,897
Butan-1-ol	λ_{max} (nm)	590	592	625	630	627
	Extinction coefficient (L mol^{-1} cm^{-1})	85,894	57,553	29,445	29,101	49,957

There are two possible products formed, the carbinol and the leuco form of the dye, further degradation pathways are possible but this requires a longer time frame than what this studied was conducted over. These other degradation products have been used to help with forensics (56). Table 15, provides the extinction coefficients as found by Lewis, et al.

Table 15: Extinction coefficients as found by Lewis, et al. (1).

		Crystal violet	Ethyl violet	Victoria blue R
Methanol	λ_{max} (nm)	586	590	578
	Extinction coefficient (L mol^{-1} cm^{-1})	109,000	106,000	74,000
Ethanol	λ_{max} (nm)	589	591	574
	Extinction coefficient (L mol^{-1} cm^{-1})	104,000	101,000	74,000
Propan-1-ol	λ_{max} (nm)	589	592	573
	Extinction coefficient (L mol^{-1} cm^{-1})	106,000	101,000	72,000
Butan-1-ol	λ_{max} (nm)	589	593	573
	Extinction coefficient (L mol^{-1} cm^{-1})	100,000	99,000	71,000
Water	λ_{max} (nm)	590	595	611
	Extinction coefficient (L mol^{-1} cm^{-1})	95,000	92,000	81,000

The difference between the values of the extinction coefficients in Tables 14 and 15 relate to the purity of the dyes. This has been discussed in the purity section. However, it may be more appropriate to suggest that the assumption made in the purity section of the all dyes been of purity which is greater than 90% may not hold entirely true or corresponds to the manufactures specifications. This comparison can be made with crystal violet where it would be more appropriate to suggest that the Acros Organics dye has a purity of greater than 80%. Since the main objective of this work relates to the relative position off the peaks in the absorption spectrum, this does not affect the interpretation of the results.

Malachite green is reported to have a higher extinction coefficient of 148,900 L mol^{-1} cm^{-1} (43), but it is unknown which solvent this was obtained in. It can be confirmed from this study that both malachite green and brilliant green produce higher extinction coefficient values. It is unclear currently as to why malachite green and brilliant green produce higher extinction coefficients.

To understand fully how the extinction coefficients of the dyes can provide information on the solvent interactions and solvation properties would require further work.

Conclusions

This study set out to validate the theories behind the shoulder present on the absorbance spectra of triarlymethane dyes. To do this, three objectives were set to achieve the aim.

The first objective involved the manipulation of the absorbance spectrum, this was completed, via a series of experiments in which the solvent was changed and also studied at 4 other temperatures other than room temperature.

The second objective was to determine how/if symmetry plays a role in the presence of the shoulder. The use of group theory was employed to achieve this objective.

Finally, objective 3 uses the results from objective 1 and 2 which have been discussed throughout this document to see if one or more of the theories holds more precedence.

The results from this study, have found that the solvent interacts with the dyes crystal violet, ethyl violet, malachite green and brilliant green, in two ways. Firstly, via interaction with the central carbon, this results in one of the phenyl rings rotating in the complete opposite direction to the others. Secondly by hydrogen bonding with the nitrogen, this causes the phenyl ring to rotate to be in the plane of the molecule. Both interactions result in a reduction in the symmetry of the dyes. Victoria blue R, shows that the interaction is from a hydrogen on one of the nitrogen's.

Further to the solvent interactions, with the dyes were backed by the temperature results. The degree of splitting found to decreases as temperature decreased. The temperature raises the possibility that temperature may affect solvation and solvatochromic parameters or may subsequently have a direct relationship with the dye.

The initial analysis done on extinction coefficients, helps aid the understanding that the solvent is interacting with the dye and will have an effect on the absorbance value produced. Though the extinction coefficients was not a primary objective of this study and further work would be required.

Overall, this study strengthens the idea from literature that symmetry breaking is the cause of the secondary peak (shoulder). To further add to this Figure provides an overview of the potential causes of the reduction in symmetry (breaking).

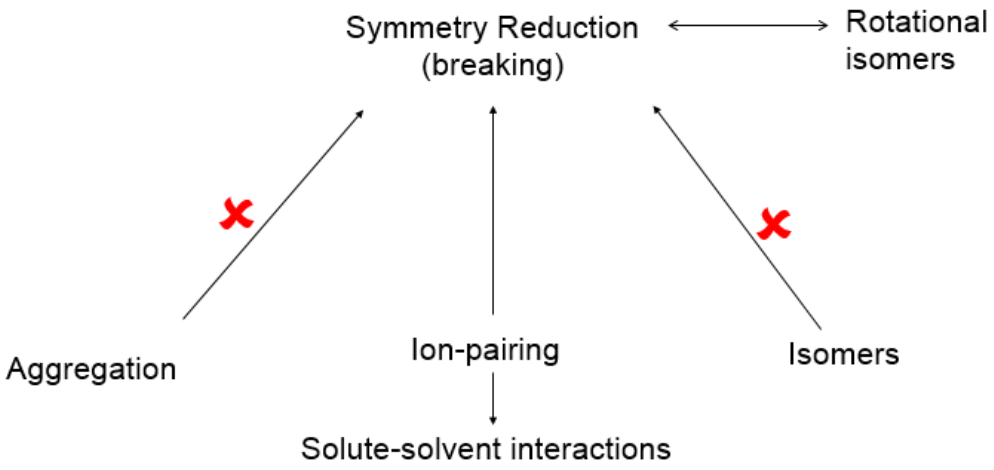

Figure 59: Diagram showing the theory holding precedence from this dissertation conducted.

The reduction in symmetry is caused due to solute-solvent interactions (ion-pairing) as provided in Figure 59. This study has suggested that the concentrations used are two low for aggregation to occur. Isomers overall seems to be more a mis-interpretation of terminology. However, rotational isomers seem to be the same as symmetry reduction (breaking) it's just another way of looking at it.

Figure 59, holds for this study conducted. The main limitation of this study is due to the small scope where concentration and pressure effects have not been accounted for.

Further studies need to be carried out to validate the theory behind the secondary peak with regards to all parameters which influence the absorbance spectrum. Also, a natural progression of this work would be to further analyse the relationship between temperature and solvent or temperature and dye. Finally, further research might explore the relationship between dye extinction coefficient and solvent.

Acknowledgements

The following acknowledgements would like to be made to: Dr R Lowry for his invaluable help and support throughout the development of this dissertation as project advisor: Andy Arnold for his support in the laboratory when using the photodiode array spectrophotometer. Dr Jeremy Clark, for supplying and maintenance of the thermocouple used. Duncan Rose, at Sigma Aldrich who provided information about the dyes that were supplied by the company.

References

1. Lewis, L, M., Indig, G, L. Solvent effects on the spectroscopic properties of triarylmethane dyes. Dyes and Pigments. 2000;46(3):145-54.
2. Venkataraman, K. The Analytical Chemistry of Synthetic Dyes. United states of America: Wiley & Sons, Inc; 1977.
3. Oliveira, C, S., Branco, K P., Baptista, M, S., Indig, G, L. Solvent and concentration effects on the visible spectra of tri-para-dialkylamino-substituted triarylmethane dyes in liquid solutions. Spectrochimica Acta Part a-Molecular and Biomolecular Spectroscopy. 2002;58(13):2971-82.
4. Duxbury D, F. The Photochemistry and Photophysics of Triphenylmethane Dyes in Solid and Liquid-Media. Chemical Reviews. 1993;93(1):381-433.
5. Zollinger, H. Color chemistry: syntheses, properties, and applications of organic dyes and pigments. 2nd ed. ed: VCH; 1991.
6. Gürses A., Açıkyıldız M, G., Kübra. Gürses, M. Sadi. Dyes and Pigments: Their Structure and Properties. Springer; 2016.
7. Sharp D, W, A. The Penguin Dictionary of Chemistry. London: Penguin Group; 1983.
8. Brooker, L, G, S., White, F, L. Steric hindrance to planarity in dye molecules. Chemical reviews. 1947;41(2):325.
9. Griffiths, J. Recent Developments in the Colour and Constitution of Organic Dyes. Coloration Technology. 1981;11:37-57.
10. Lubai, C., Xing, C., Yufen, H., Griffiths, J. An Approach to the Prediction of Absorption Bandwidths of Dyes using the PPP-MO Procedure. Dyes and pigments. 1989;10:123-40.
11. Chan, C, C., Lam H., Lee Y, C, Z., Hang X. Analytical Method Validation and Instrument Performance Verification. United States of America: John Wiley & Sons, Inc.; 2004.
12. Robinson, D, Z. Quantitative Analysis with Infrared Spectrophotometers. Analytical Chemistry. 1952;24(4):619-22.
13. Kenkel, J. Analytical Chemistry for Technicians. 4th ed. New York: CRC Press; 2014.
14. Jones, D, G. Photodiode Array Detectors in UV-VIS Spectroscopy: Part 1. Analytical chemistry. 1985;57(9):1057-73.
15. Perkampus, H-H. UV-VIS Spectroscopy and It's Applications: Springer Laboratory; 1992.
16. Adams, E, Q., Rosenstein L. The Colour and Ionization of Crystal-violet. Journal of the American Chemical Society. 1914;36(7):1452-73.
17. Korppitommola, J, Yip, R, W. Solvent Effects on the Visible Absorption-Spectrum of Crystal Violet. Canadian Journal of Chemistry-Revue Canadienne De Chimie. 1981;59(2):191-4.

18. Lewis, G, N., Bigeleisen, J. The Second Order x Bands in Absorption Spectra. Journal of American Chemical Society. 1943;65(11):2107-10.

19. Lewis, G, N. Rules for the Absorption Spectra of Dyes. Journal of American Chemical Society. 1945;67(5):770-5.

20. Guinot, S, G, R., Hepworth, J, D., Wainwright, M. The effects of cyclic terminal groups in di- and tri-arylmethane dyes. Part 2. Steric and electronic effects in derivatives of Victoria Blue. Journal of the Chemical Society-Perkin Transactions 2. 1998(2):297-303.

21. Lewis, G, N., Magel, T, T., Lipkin, D. Isomers of Crystal Violet ion. Their Absorption and Re-emission of Light. Journal of the American Chemical Society. 1942;64(8):1774-82.

22. Maruyama Y., Ishikawa, M., Satozono, H. Femtosecond isomerization of crystal violet in alcohols. Journal of the American Chemical Society. 1996;118(26):6257-63.

23. Clark F, T., Drickamer H, G. High-Pressure Studies of Rotational-Isomerism of Triphenylmethane Dye Molecules. Chemical Physics Letters. 1985;115(2):173-5.

24. Clark F, T., Drickamer H, G. High-Pressure Study of Triphenylmethane Dyes in Polymeric and Aqueous-Media. Journal of Physical Chemistry. 1986;90(4):589-92.

25. Barker C, C., Bride M, H., Stamp, A. Steric Effects in Di- and Tri-arylmethnes. Part I. Electronic Absorption Spectra of 0- Methyl Derivatives of Michler's Hydrol Blue and Crystal Violet; Conformational Isomers of Crystal Violet. . Journal of the Chemical Society. 1959:3957- 63.

26. Lueck, H, B., Rice, B, L., McHale, J, L. Aggregation of Triphenylmethane Dyes in Aqueous-Solution - Dimerization and Trimerization of Crystal Violet and Ethyl Violet. Spectrochimica Acta Part a-Molecular and Biomolecular Spectroscopy. 1992;48(6):819-28.

27. Ghanadzadeh, A., Zeini, A., Kashef, A. Environment effect on the electronic absorption spectra of crystal violet. Journal of Molecular Liquids. 2007;133(1-3):61-7.

28. Loison, C., Antoine, R., Broyer, M., Dugourd, P., Guthmuller, J., Simon, D. Microsolvation effects on the optical properties of crystal violet. Chemistry-a European Journal. 2008;14(24):7351-7.

29. McKay R, B., Hillson P, J. Metachromatic Behaviour of Dyes in SolutionInterpretation on the Basis of Interaction between Dye Ions and Counter-ions. Transactions of the Faraday Society. 1965;61:1800-10.

30. Chen, D, T, Y., Laidler K, J. Pressure and Temperature Effects on the Kinetics of the Alkaline Fading of Organic Dyes in Aqueous Solution. Canadian Journal of Chemistry. 1959;37(3):599-612.

31. Sheppard S, E., Geddes A, L. Effect of Solvents upon the Absorption Spectra of Dyes. IV. Water as Solvent: A Common Pattern. Journal of the American Chemical Society. 1944;66(12):1995-2002.

32. Hopkinson A, C., Wyatt, P, A, H. Substituent Effects on Electronic Absorption Spectra of Phenolphthalein and Phenolsulphonpthalein Monopositive Ions. Journal of the Chemical Society B-Physical Organic. 1970(3):530-535.

33. Lewis G, N., Bigeleisen J. The y bands in Absorption Spectra. Journal of American Chemical Society. 1943;65(11):2102-6.

34. Lueck H, B., McHale J, L., Edwards N, D. Symmetry-breaking solvent effects on the electronic structure and spectra of a Series of triphenylmethane dyes. Journal of American Chemical Society. 1992;144(7):2342-8.

35. Lueck, H, B., Daniel, D, C., McHale, J, L. Resonance Raman-Study of Solvent Effects on a Series of Triarylmethane Dyes. Journal of Raman Spectroscopy. 1993;24(6):363-70.

36. Lovell, S., Marquardt B,J., Kahr, B. Crystal violet's shoulder. Journal of the Chemical Society-Perkin Transactions 2. 1999(11):2241-7.

37. Benamotz, D., Harris, C, B. Ground-State and Excited-State Torsional Dynamics of a Triphenylmethane Dye in Low-Viscosity Solvents. Chemical Physics Letters. 1985;119(4):305-11.

38. Brindle, I., Jones, A, M. Electronically asymmetric triphenylmethane dyes. Half-methoxy analogues of Malachite Green. Dyes and Pigments. 2000;47(1-2):117-27.

39. Campo, J., Painelli A, Terenziani F, Van Regemorter T, Beljonne D, Goovaerts E, et al. First Hyperpolarizability Dispersion of the Octupolar Molecule Crystal Violet: Multiple Resonances and Vibrational and Solvation Effects. Journal of the American Chemical Society. 2010;132(46):16467-78.

40. Karukstis, K.K., Gulledge, A, V. Analysis of the solvatochromic behavior of the disubstituted triphenylmethane dye Brilliant Green. Analytical Chemistry. 1998;70(19):4212-7.

41. Giles, C, H., Greczek, J, J. A Review of Methods of Purifying and Analyzing Water-Soluble Dyes. Textile Research Journal. 1962;32(6):506-15.

42. Horobin, R, W., Kiernan, J, A. CONN'S Biological Stains A Handbook of Dyes, Stains and Fluorochromes for Use in Biology and Medicine. 10th ed. Oxford: BIOS Scientific Publishers; 2002.

43. Green, F. The Sigma-Aldrich Handbook of Stains, Dyes and Indicators. United States of America: Aldrich Chemical Company, Inc.; 1990.

44. Sigma Aldrich (online). 2018. Available at: https://www.sigmaaldrich.com/united-kingdom.html (Accessed on: 28/02/18)

45. Vincent, A. Molecular Symmetry and Group Theory. 2nd ed. Chichester: John Wiley & Sons, LTD; 2001.

46. Suzuki, H. Electronic Absorption Spectra and Geometry of Organic Molecules: An Application of Molecular Orbital Theory. London: Academic Press INC.; 1967.

47. Galban, .J, de Marcos, .S, Sanz, .I, Ubide, C., Zuriarrain, J. Uncertainty in modern spectrophotometers. Analytical Chemistry. 2007;79(13):4763-7.

48. Ellison, S, L, R., Williams, A. Eurachem/CITAC guide: Quantifying Uncertainty in Analytical Measurement 2012. Available from: www.eurachem.org.

49. Soovali, L., Room, EI., Kutt, A., Kaljurand, .I, Leito, I. Uncertainty sources in UV-Vis spectrophotometric measurement. Accreditation and Quality Assurance. 2006;11(5):246-55.

50. Chulvi, K., Costero, A, M., Ochando, L, E., Gil, S., Vivancos, J, L., Gavina P. Solvatochromic and Single Crystal Studies of Two Neutral Triarylmethane Dyes with a Quinone Methide Structure. Molecules. 2015;20(11):20688-98.

51. deJuan, A., Fonrodona, G., Casassas, E. Solvent classification based on solvatochromic parameters: A comparison with the Snyder approach. Trac-Trends in Analytical Chemistry. 1997;16(1):52-62.

52. Lide D, R. CRC Handbook of Chemistry and Physics. 85th ed. Florida: CRC Press; 2004.

53. Kamlet, M, J., Abboud, J, L., Taft, R, W. Solvatochromic Comparison Method .6. Pi-Star Scale of Solvent Polarities. Journal of the American Chemical Society. 1977;99(18):6027-38.

54. Korppitommola, J., Kolehmainen, E., Salo, E., Yip, R, W. The Temperature-Dependent Red-Shift of the Visible Absorption-Spectra of Crystal Violet in Alcohol-Solutions. Chemical Physics Letters. 1984;104(4):373-7.

55. Brini, E., Fennell, C, .J, Fernandez-Serra, M., Hribar-Lee, B., Luksic, M., Dill, K, A. How Water's Properties Are Encoded in Its Molecular Structure and Energies. Chemical Reviews. 2017;117(19):12385-414.

56. Weyermann, C., Kirsch, D., Vera, C, C., Spengler, B. Evaluation of the Photodegradation of Crystal Violet upon Light Exposure by Mass Spectrometric and Spectroscopic Methods. Journal of Forensic Sciences. 2009;54(2):339-45.